Optimization of Synthesis Oversampled Complex Filter Banks

Jérôme Gauthier, *Member, IEEE*, Laurent Duval, *Member, IEEE*, and Jean-Christophe Pesquet, *Senior Member, IEEE*

***Abstract*—An important issue with oversampled FIR analysis filter banks (FBs) is to determine inverse synthesis FBs, when they exist. Given any complex oversampled FIR analysis FB, we first provide an algorithm to determine whether there exists an inverse FIR synthesis system. We also provide a method to ensure the Hermitian symmetry property on the synthesis side, which is serviceable to processing real-valued signals. As an invertible analysis scheme corresponds to a redundant decomposition, there is no unique inverse FB. Given a particular solution, we parameterize the whole family of inverses through a null space projection. The resulting reduced parameter set simplifies design procedures, since the perfect reconstruction constrained optimization problem is recast as an unconstrained optimization problem. The design of optimized synthesis FBs based on time or frequency localization criteria is then investigated, using a simple yet efficient gradient algorithm.**

***Index Terms*—Filter design, frequency localization, inversion, lapped transforms, modulated filter banks, optimization, oversampled filter banks, time localization.**

I. Introduction

SINCE the 1970s, filter banks (FBs) have become a central tool in signal/image processing and communications: lapped or discrete wavelet transforms can be viewed as instances of FB structures. Likewise, oversampled FBs (OFBs) constitute an extensively studied instance with remaining open questions. Their development came along under a variety of different appellations, to name a few: general analysis-synthesis systems [1], discrete Fourier transform (DFT) with stack-shift capability, overlap-add or generalized DFT, underdecimated systems, oversampled harmonic modulated filter banks [2], [3], complex lapped transforms [4], generalized lapped pseudo-biorthogonal transform, etc.

In a more generic form, OFBs have received a considerable attention both theoretically and in many applications, in the past 10 years, following their association with specific types of frames [2], [5], [6]. Their design flexibility, improved frequency selectivity and increased robustness to noise and aliasing distortions have made them useful for subband adaptive filtering in audio processing [7], noise shaping [8], denoising [3], multiple description coding [9], echo cancellation [10], multiple antenna code design [11], channel equalization [12]–[14], or channel coding [15].

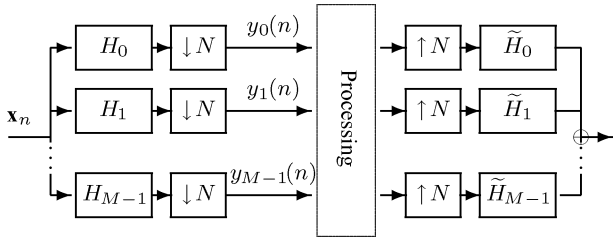

Fig. 1. Oversampled M-channel filter bank.

Two major problems arise when resorting to OFBs: i) the existence of an inverse for the analysis OFB achieving perfect reconstruction (PR) and ii) the determination of an "optimal" synthesis FB. Since the additional degrees of freedom gained through redundancy may increase the design complexity, several works have focused on FBs modulated with a single [16], [17] or multiple windows [18]. More general formulations are based on factorizations of OFB polyphase representations with additional constraints (restricted oversampling ratios, symmetry, realness, or filter length) into a lattice [19]–[22] or a lifting structure [23]. Constructions with near perfect reconstruction (relaxing the PR property) have also been proposed [10], [24]–[26]. In [27]–[29], more involved algebraic tools (such as Gröbner bases) have also been employed. Recently, Chai *et al.* have proposed a design based on FB state-space representations [30]. The design may use different kinds of optimization criteria based on filter regularity or more traditional cost functions based on filter shape (subband attenuation [10], [21], coding gain [31]). Most of those synthesis FB designs rely on minimum-norm solutions. An interesting approach combining the latters with a null space method was successfully pursued by Mansour [32] for synthesis window shape optimization in a modulated DFT FB.

Within the compass of the proposed work is a relatively generic construction and optimization of oversampled synthesis filter banks with finite impulse response (FIR) properties at both the analysis and synthesis sides. We can additionally impose a practically useful Hermitian symmetry on the synthesis side. This work extends the results given in two previous conference papers [33], [34]. A special case has been judiciously devised in [22], for specific filter length and redundancy factor

Manuscript received July 28, 2008; accepted April 20, 2009. First published May 27, 2009; current version published September 16, 2009. The associate editor coordinating the review of this manuscript and approving it for publication was Prof. Gerald Schuller.

J. Gauthier and J.-C. Pesquet are with the Laboratoire d'Informatique Gaspard Monge CNRS-UMR 8049, Université Paris-Est, 77454 Marne-la-Vallée Cedex 2, France (e-mail: jerome.gauthier@univ-paris-est.fr; jean-christophe.pesquet@univ-paris-est.fr).

L. Duval is with the Institut Français du Pétrole, IFP, Technology, Computer Science and Applied Mathematics Division, 92852 Rueil-Malmaison, France (e-mail: laurent.duval@ifp.fr).

Color versions of one or more of the figures in this paper are available online at http://ieeexplore.ieee.org.

Digital Object Identifier 10.1109/TSP.2009.2023947

allowing closed form expressions for two design criteria. In Section II, we recall the polyphase notation used throughout this paper. Given arbitrary FIR complex oversampled analysis FB, we first describe in Section III-A a simple algorithm to test whether it is FIR invertible or not, based on known results on polynomial matrices [35], [36]. The standard Moore-Penrose pseudoinverse (PI) solution [37] is studied in Section III-B. In Section III-C, a method is supplied to enforce an Hermitian symmetric FB, which is useful for real data analysis, processing and synthesis. In Section IV, the problem of the optimal design of the synthesis FB is addressed. Although optimization can be studied both on the analysis and synthesis sides [38], [39], we consider here a given analysis FB and work on the synthesis side. We derive in Section IV-A an efficient parameter set size reduction for this purpose. Using time or frequency localization criteria, we then reformulate in Section IV-B the constrained optimization problem as an unconstrained one for both the general and Hermitian symmetric cases. After describing the optimization process, we illustrate, in Section V, the different methods proposed for the inversion and optimization on three classical oversampled real and complex FB types.

II. Problem Statement

A. Notations

Lapped transforms [40] were introduced in [41] to avoid blocking artifacts in audio processing. Similarly for images, they reduce tiling effects produced by classical block transforms (as can be seen in the JPEG image compression format). Lapped transforms belong to the class of FBs, such as the one represented in Fig. 1, with a decimation factor N smaller than the length of each filter. The filters, whose impulse responses are denoted by $(h_i)_{0\leq i<M}$, are supposed of finite length kN with k an integer greater than or equal to 2. We therefore consider k overlapping blocks of size N.

A signal $(x(n))_{n\in\mathbb{Z}}$ is decomposed by M filters; since the decimation factor is N, the overall redundancy of the transform is $M/N = k'$. In this paper, we investigate the oversampled case, i.e., $k' > 1$. The M outputs of the analysis FB are denoted by $(y_i(n))_{0\leq i<M}$. With these notations, the outputs of the analysis FB are expressed, for all $i \in \{0,\dots,M-1\}$ and $n \in \mathbb{Z}$, as

$$y_i(n) = \sum_p h_i(p)x(Nn-p) = \sum_\ell \sum_{j=0}^{N-1} h_i(N\ell+j)x\left(N(n-\ell)-j\right). \quad (1)$$

B. Polyphase Formulation

Let $\boldsymbol{H}(\ell) = [h_i(N\ell+j)]_{0\leq i<M,0\leq j<N}$, $\ell \in \{0,\dots,k-1\}$ be the k polyphase matrices obtained from the impulse responses of the analysis filters. We also define: $\forall n \in \mathbb{Z}$, $\mathbf{x}(n) = (x(Nn-j))_{0\leq j<N}$, the polyphase vector from the input signal $x(n)$, leading to concisely rewriting (1) into a convolutive form

$$\mathbf{y}(n) = (y_0(n),\dots,y_{M-1}(n))^\top = \sum_{\ell=0}^{k-1} \boldsymbol{H}(\ell)\mathbf{x}(n-\ell) = (\boldsymbol{H} * \mathbf{x})(n) \quad (2)$$

where $^\top$ is the transpose operator. Thus, (2) can be reexpressed as: $\mathbf{y}[z] = \boldsymbol{H}[z]\mathbf{x}[z]$, where $\boldsymbol{H}[z] = \sum_{\ell=0}^{k-1} \boldsymbol{H}(\ell)z^{-\ell}$ is the $M \times N$ polyphase transfer matrix of the analysis FB and $\mathbf{x}[z]$ (respectively, $\mathbf{y}[z]$) is the z-transform of $(\mathbf{x}(n))_{n\in\mathbb{Z}}$ (respectively, $(\mathbf{y}(n))_{n\in\mathbb{Z}}$).

C. Synthesis FB

The polyphase transfer matrix of the synthesis FB: $\widetilde{\boldsymbol{H}}[z] = \sum_\ell \widetilde{\boldsymbol{H}}(\ell)z^{-\ell}$, satisfies

$$\widetilde{\mathbf{x}}[z] = \widetilde{\boldsymbol{H}}[z]\mathbf{y}[z] \quad (3)$$

where the polyphase vector of the output signal of the synthesis FB $(\widetilde{\mathbf{x}}(n))_{n\in\mathbb{Z}}$ is defined similarly to $(\mathbf{x}(n))_{n\in\mathbb{Z}}$. We deduce from (3) that $\forall n \in \mathbb{Z}, \forall i \in \{0,\dots,N-1\}$

$$\widetilde{x}(nN-i) = \sum_{j=0}^{M-1} \sum_{\ell=-\infty}^{\infty} \widetilde{H}_{i,j}(n-\ell)y_j(\ell) \quad (4)$$

where $\widetilde{\boldsymbol{H}}(\ell) = (\widetilde{H}_{i,j}(\ell))_{0\leq i<N,0\leq j<M}$. Expressing (4) with impulse responses, we can write: for every $i \in \{0,\dots,N-1\}$ and $n \in \mathbb{Z}$,

$$\widetilde{x}(nN-i) = \sum_{j=0}^{M-1} \sum_{\ell=-\infty}^{\infty} \widetilde{h}_j\left(N(n-\ell)-i\right) y_j(\ell) \quad (5)$$

which, by identifying (4) and (5), allows us to deduce that

$$\widetilde{\boldsymbol{H}}(\ell) = \left[\widetilde{h}_j(N\ell-i)\right]_{0\leq i<N,0\leq j<M}, \quad \ell \in \mathbb{Z}. \quad (6)$$

These expressions hold for any oversampled FIR FB.

III. Inversion

A. Invertibility of an Analysis FB

This work being focused on the construction of FIR synthesis filters, a preliminary point is the verification of the given analysis FB FIR invertibility. The polyphase representation of FBs offers the advantage of relating the perfect reconstruction property to the invertibility of the polyphase transfer matrix [42]. The latter matrix belongs to the ring $\mathbb{C}[z,z^{-1}]^{M\times N}$ of Laurent polynomial matrices of dimensions $M \times N$. We emphasize that we do not look for any inverse MIMO filter, but for an inverse *polynomial* matrix in $\mathbb{C}[z,z^{-1}]^{N\times M}$ instead. In other words, we aim at obtaining a (nonnecessarily causal) FIR synthesis FB.

A first answer to this FIR invertibility problem can be conveyed through the study of the Smith McMillan form of a poly-

nomial matrix [42], [43], but unfortunately this decomposition is quite costly. Park, Kalker, and Vetterli also devised a method using Gröbner bases [28] to study the invertibility of polynomial matrices which is applicable to the general multidimensional case. We describe here an alternative cost-effective method in the one-dimensional case. The following result gives a necessary and sufficient condition for a matrix to be left invertible, and, thus, for the existence of such an inverse system: let $\boldsymbol{H}[z] \in \mathbb{C}[z, z^{-1}]^{M\times N}$ be a polynomial matrix with $M > N$. The following conditions are equivalent:

1) $\boldsymbol{H}[z]$ is "coprime," which means that the determinants of the maximum minors (sub-matrices of size $N \times N$) are mutually relatively prime;
2) $\boldsymbol{H}[z]$ is left invertible in the sense that there exists $\widetilde{\boldsymbol{H}}[z] \in \mathbb{C}[z, z^{-1}]^{N\times M}$ such that $\widetilde{\boldsymbol{H}}[z]\boldsymbol{H}[z] = \boldsymbol{I}_N$.

A proof of this result can be found in [35] for instance.

The first condition is directly applicable in practice to resolve the left invertibility of the polyphase transfer matrix. Using the following procedure, we can check numerically whether this condition is satisfied.

1) Extract a maximal submatrix $\boldsymbol{H}_e[z]$ of $\boldsymbol{H}[z]$.
2) Compute $\det(\boldsymbol{H}_e[z])$, and determine its set of roots $\mathcal{S}_e$.
3) Consider another maximal submatrix. Remove from $\mathcal{S}_e$ the elements which are not roots of the determinant of this submatrix.
4) Repeat step 3) until $\mathcal{S}_e = \emptyset$ or all maximal sub-matrices have been extracted.
5) If $\mathcal{S}_e = \emptyset$ then the polyphase transfer matrix is left-invertible; otherwise, it is not.

The corresponding algorithm is easily implemented, leading to extract the roots of a single polynomial and check the roots of at most $\binom{M}{N} - 1 = (M!/N!(M-N)!) - 1$ polynomials. If the polyphase matrix is left invertible, the number of considered polynomials in practice is usually much smaller than $\binom{M}{N} - 1$, this bound being reached only when the matrix is not invertible. Note that in the case of causal filters (i.e. both $\boldsymbol{H}[z]$ and $\widetilde{\boldsymbol{H}}[z]$ are polynomial matrices in $\mathbb{C}[z^{-1}]^{N\times M}$), simpler invertibility conditions exist by invoking the so-called *column-reduced* property [44], [45]. Also notice that, one of the advantages of this algorithm over other methods is that it can be fully numerically implemented.

B. Computation of an Inverse FB

The method proposed in Section III-A only guarantees the existence of a left-inverse, corresponding to an FIR synthesis FB. Since it does not provide a constructive expression, we now perform the actual computation of an inverse polyphase transfer matrix. We assume hereafter that $\boldsymbol{H}[z]$ was proven to be FIR left invertible.

Since the goal is to achieve PR, we search for a matrix $\widetilde{\boldsymbol{H}}[z]$ in $\mathbb{C}[z, z^{-1}]^{N\times M}$ such that $\widetilde{\boldsymbol{H}}[z]\boldsymbol{H}[z] = \boldsymbol{I}_N$ and there exists $(p_1, p_2) \in \mathbb{N}^2$ such that the polyphase transfer function of the synthesis FB reads: $\widetilde{\boldsymbol{H}}[z] = \sum_{\ell=-p_1}^{p_2} \widetilde{\boldsymbol{H}}(\ell) z^{-\ell}$. The resulting overlapping factor of the synthesis filters is $p = p_1 + p_2 + 1$. When working with Laurent polynomial matrices, these integers p_1 and p_2 are *a priori* unknown, whereas with polynomial matrices a bound exists [44]. By rewriting the PR property in block convolutional form, we get the following linear system:

$$\mathcal{H}\widetilde{\mathcal{H}} = \mathcal{U} \tag{7}$$

where

$$\begin{aligned}\widetilde{\mathcal{H}}^\top &= \left[\widetilde{\boldsymbol{H}}(-p_1), \ldots, \widetilde{\boldsymbol{H}}(p_2)\right] \in \mathbb{C}^{N\times pM} \\ \mathcal{U}^\top &= \left[\boldsymbol{0}_{N,p_1N}, \boldsymbol{I}_N, \boldsymbol{0}_{N,(p_2+k-1)N}\right] \in \mathbb{R}^{N\times(k+p-1)N},\end{aligned} \tag{8}$$

and

$$\mathcal{H}^\top = \begin{pmatrix} \boldsymbol{H}(0) & \cdots & \boldsymbol{H}(k-1) & & 0 \\ & \ddots & & \ddots & \\ 0 & & \boldsymbol{H}(0) & \cdots & \boldsymbol{H}(k-1) \end{pmatrix} \in \mathbb{C}^{pM\times(k+p-1)N}. \tag{9}$$

As aforementioned, p_1 and p_2 are unknown, but since the system (7) is supposed invertible, at least a couple of integers (p_1, p_2) solving the system exists. The values of p_1 and p_2 are actually obtained by increasing the value of p and looking for every couple satisfying $p = p_1 + p_2 + 1$, starting with $p = 1$. Hence, for a given p, we consider all (p_1, p_2) in $\{(p-1, 0), (p-2, 1), \ldots, (0, p-1)\}$. The first p allowing a Moore-Penrose pseudoinverse [46] solution to (7) provides an inverse polyphase transfer matrix of minimum order.

C. Hermitian Symmetric Case

1) Symmetry Conditions: It is well known that the Fourier transform of a real signal is Hermitian Symmetric (HS): its frequency decomposition is symmetric for the real part and antisymmetric for the imaginary part. Conversely, if the coefficients are HS in the frequency domain, then the reconstructed signal is real. This property is very useful for real data filtering, which often consists of removing or thresholding coefficients in the frequency domain before reconstructing. Securing the reconstruction of real-valued signals from the transformed coefficients is thus a desirable property. In this section, we study the HS case and its effects on the methods proposed in the previous sections.

The HS property in the synthesis filters is satisfied provided that, considering any symmetric subband indices $j_f \in \{0, \ldots, M-1\}$ and $M - 1 - j_f$, for any coefficients $(y_i(n))_{0\le i<M}$ such that $y_i(n) = 0$ if $(i, n) \neq (j_f, n_f)$ or $(i, n) \neq (M-1-j_f, n_f)$ with $n_f \in \mathbb{Z}$ and, such that $y_{j_f}(n_f) = y_{M-1-j_f}(n_f)$, a real-valued signal is reconstructed. The reconstructed signal reads

$$\begin{aligned}\widetilde{x}(m) &= \sum_{j=0}^{M-1} \sum_{\ell=-\infty}^{\infty} \widetilde{h}_j(m - N\ell) y_j(\ell) \\ &= \widetilde{h}_{j_f}(m - n_f N) y_{j_f}(n_f) \\ &\quad + \widetilde{h}_{M-1-j_f}(m - n_f N)\overline{y_{j_f}(n_f)}.\end{aligned}$$

A necessary and sufficient condition for $\widetilde{x}(m) \in \mathbb{R}$ for all $y_{j_f}(n_f) \in \mathbb{C}$, is that $\widetilde{h}_{j_f}(m - n_f N) = \overline{\widetilde{h}_{M-1-j_f}(m - n_f N)}$.

This condition must be verified for any couple of integers (j_f, n_f). The condition on the synthesis filter is then: $\forall j \in \{0,\dots,M-1\}$ and $\forall n \in \mathbb{Z}$, $\widetilde{h}_j(n) = \overline{\widetilde{h}_{M-1-j}(n)}$. Using (6), we rewrite the condition as

$$\forall \ell \in \{-p_1,\dots,p_2\}, \quad \widetilde{\boldsymbol{H}}(\ell) = \overline{\widetilde{\boldsymbol{H}}(\ell)}\boldsymbol{J}_M. \tag{10}$$

where $\boldsymbol{J}_M$ is the $M \times M$ counter-identity matrix

$$\boldsymbol{J}_M = \begin{pmatrix} 0 & & 1 \\ & \iddots & \\ 1 & & 0 \end{pmatrix}.$$

We have supposed here that the transformed coefficients of a real signal exhibit the HS property. In other words, for any real signal $(x(n))_{n\in\mathbb{Z}}$, and for any couple $(j_f, n_f) \in \{0,\dots,M-1\}\times\mathbb{Z}$, the output of the analysis FB verifies: $y_{j_f}(n_f) = \overline{y_{M-j_f-1}(n_f)}$. This condition can be rewritten

$$\sum_m h_{j_f}(m)x(Nn_f - m) = \sum_m \overline{h_{M-j_f-1}(m)}x(Nn_f - m).$$

Considering a zero input signal x except for one sample, we deduce that $h_{j_f}(n) = \overline{h_{M-j_f-1}}(n)$, which is equivalent to

$$\boldsymbol{H}(\ell) = \boldsymbol{J}_M\overline{\boldsymbol{H}(\ell)}. \tag{11}$$

Hence, if the analysis FB verifies Condition (11), then the coefficients after decomposition satisfy the HS property.

Remark 1: Consider an invertible HS analysis FB. By inserting (11) in the PR condition we get

$$\delta_\ell \boldsymbol{I}_N = \sum_{s=\max(\ell-k+1,-p_1)}^{\min(p_2,\ell)} \overline{\widetilde{\boldsymbol{H}}(s)}\boldsymbol{J}_M\boldsymbol{H}(\ell-s).$$

It implies that if $\widetilde{\mathcal{H}} = [\widetilde{\boldsymbol{H}}(-p_1),\dots,\widetilde{\boldsymbol{H}}(p_2)]^\top$ is a solution of the linear system (7) then, under the HS hypothesis on the analysis FB, $\widetilde{\mathcal{H}_2} = [\overline{\widetilde{\boldsymbol{H}}(-p_1)}\boldsymbol{J}_M,\dots,\overline{\widetilde{\boldsymbol{H}}(p_2)}\boldsymbol{J}_M]^\top$ is also a solution of the linear system. Finally, it follows that the sum: $\widetilde{\mathcal{H}_0} = (1/2)(\widetilde{\mathcal{H}} + \widetilde{\mathcal{H}_2})$ is also a solution. Moreover, this solution verifies Condition (10) by construction.

In other words, we have proved that an invertible HS analysis FB admits at least one HS synthesis FB.

2) Construction Method: We suppose here that the analysis FB was proven invertible and that the matrices $\boldsymbol{H}(\ell)$ satisfy Condition (11). Our objective is to build a synthesis FB possessing both the PR and HS properties.

a) First case: M is even: First, we rewrite (10) and (11)

$$(10) \Leftrightarrow \forall \ell \in \{-p_1,\dots,p_2\}, \begin{cases} \widetilde{\boldsymbol{H}}(\ell) = \left[\widetilde{\boldsymbol{H}_1}(\ell), \widetilde{\boldsymbol{H}_2}(\ell)\right], \\ \widetilde{\boldsymbol{H}_1}(\ell) = \overline{\widetilde{\boldsymbol{H}_2}(\ell)}\boldsymbol{J}_{M'} \\ \quad \text{with } \widetilde{\boldsymbol{H}_1} \in \mathbb{C}^{N\times M'} \text{ and } \widetilde{\boldsymbol{H}_2} \in \mathbb{C}^{N\times M'}, \end{cases}$$

$$(11) \Leftrightarrow \forall \ell \in \{0,\dots,k-1\}, \begin{cases} \boldsymbol{H}(\ell) = \begin{pmatrix} \boldsymbol{H}_1(\ell) \\ \boldsymbol{H}_2(\ell) \end{pmatrix} \\ \boldsymbol{H}_1(\ell) = \boldsymbol{J}_{M'}\overline{\boldsymbol{H}_2(\ell)} \\ \quad \text{with } \boldsymbol{H}_1 \in \mathbb{C}^{M'\times N} \text{ and } \boldsymbol{H}_2 \in \mathbb{C}^{M'\times N} \end{cases}$$

with $M' = M/2$. Combining these conditions and the PR property, we get

$$\delta_\ell \boldsymbol{I}_N = \sum_{s=\max(\ell-k+1,-p_1)}^{\min(p_2,\ell)} \widetilde{\boldsymbol{H}_1}(s)\boldsymbol{H}_1(\ell-s) + \sum_{s=\max(\ell-k+1,-p_1)}^{\min(p_2,\ell)} \overline{\widetilde{\boldsymbol{H}_1}(s)}\boldsymbol{J}_{M'}^2\overline{\boldsymbol{H}_1(\ell-s)}.$$

Since $\boldsymbol{J}_{M'}^2 = \boldsymbol{I}_{M'}$, the previous equation can be seen as the sum of a complex matrix with its conjugate, leading to a real matrix. We deduce that

$$\frac{\delta_\ell \boldsymbol{I}_N}{2} = \sum_{s=\max(\ell-k+1,-p_1)}^{\min(p_2,\ell)} \left[\widetilde{\boldsymbol{H}_1^R}(s), -\widetilde{\boldsymbol{H}_1^I}(s)\right] \begin{pmatrix} \boldsymbol{H}_1^R(\ell-s) \\ \boldsymbol{H}_1^I(\ell-s) \end{pmatrix}$$

where $\boldsymbol{A}^R$ is the matrix of the real part of a matrix $\boldsymbol{A}$ and $\boldsymbol{A}^I$ is its imaginary part. We will then define the following matrices:

$$\widetilde{\mathcal{H}_s}^\top = \left[\widetilde{\boldsymbol{H}_1^R}(-p_1), -\widetilde{\boldsymbol{H}_1^I}(-p_1),\dots,\widetilde{\boldsymbol{H}_1^R}(p_2), -\widetilde{\boldsymbol{H}_1^I}(p_2)\right] \in \mathbb{R}^{N\times pM} \tag{12}$$

and

$$\mathcal{H}_s^\top = \begin{pmatrix} \boldsymbol{H}_1^R(0) & \cdots & \boldsymbol{H}_1^R(k-1) & & 0 \\ \boldsymbol{H}_1^I(0) & \cdots & \boldsymbol{H}_1^I(k-1) & & 0 \\ & \ddots & & \ddots & \\ 0 & & \boldsymbol{H}_1^R(0) & \cdots & \boldsymbol{H}_1^R(k-1) \\ 0 & & \boldsymbol{H}_1^I(0) & \cdots & \boldsymbol{H}_1^I(k-1) \end{pmatrix} \in \mathbb{R}^{pM\times(k+p_1+p_2)N}.$$

b) Second case: M is odd: Similarly to the first case, (10) and (11) can be rewritten

$$(10) \Leftrightarrow \forall \ell \in \{-p_1,\dots,p_2\} \begin{cases} \widetilde{\boldsymbol{H}}(\ell) = \left[\widetilde{\boldsymbol{H}_1}(\ell), \mathbf{c}_1(\ell), \widetilde{\boldsymbol{H}_2}(\ell)\right] \\ \widetilde{\boldsymbol{H}_1}(\ell) = \overline{\widetilde{\boldsymbol{H}_2}(\ell)}\boldsymbol{J}_{M'} \text{ and } \mathbf{c}_1(\ell) \in \mathbb{R}^N \\ \quad \text{with } \widetilde{\boldsymbol{H}_1} \in \mathbb{C}^{N\times M'} \text{ and } \widetilde{\boldsymbol{H}_2} \in \mathbb{C}^{N\times M'}, \end{cases}$$

$$(11) \Leftrightarrow \forall \ell \in \{0,\dots,k-1\} \begin{cases} \boldsymbol{H}(\ell) = \begin{pmatrix} \boldsymbol{H}_1(\ell) \\ \mathbf{c}_2(\ell)^\top \\ \boldsymbol{H}_2(\ell) \end{pmatrix}, \\ \boldsymbol{H}_1(\ell) = \boldsymbol{J}_{M'}\overline{\boldsymbol{H}_2(\ell)} \text{ and } \mathbf{c}_2(\ell) \in \mathbb{R}^N \\ \quad \text{with } \boldsymbol{H}_1 \in \mathbb{C}^{M'\times N} \text{ and } \boldsymbol{H}_2 \in \mathbb{C}^{M'\times N} \end{cases}$$

with $M' = (M-1)/2$. Combining these conditions with the PR equation and following the same reasoning as in the previous section, we deduce that

$$\frac{\delta_\ell \boldsymbol{I}_N}{2} = \sum_{s=\max(\ell-k+1,-p_1)}^{\min(p_2,\ell)} \left[\widetilde{\boldsymbol{H}_1^R}(s), \frac{\mathbf{c}_1(s)}{\sqrt{2}}, -\widetilde{\boldsymbol{H}_1^I}(s)\right] \times \begin{pmatrix} \boldsymbol{H}_1^R(\ell-s) \\ \frac{\mathbf{c}_2(\ell-s)^\top}{\sqrt{2}} \\ \boldsymbol{H}_1^I(\ell-s) \end{pmatrix}.$$

Subsequently, we introduce in this case the following matrices:

$$\widetilde{\mathcal{H}}_s^\top = \Big[\widetilde{\boldsymbol{H}_1^R}(-p_1), \frac{\mathbf{c}_1(-p_1)}{\sqrt{2}}, -\widetilde{\boldsymbol{H}_1^I}(-p_1), \ldots, \widetilde{\boldsymbol{H}_1^R}(p_2), \frac{\mathbf{c}_1(p_2)}{\sqrt{2}}, -\widetilde{\boldsymbol{H}_1^I}(p_2)\Big] \in \mathbb{R}^{N\times pM} \quad (13)$$

and

$$\mathcal{H}_s^\top = \begin{pmatrix} \boldsymbol{H}_1^R(0) & \cdots & \boldsymbol{H}_1^R(k-1) & & 0 \\ \frac{\mathbf{c}_2(0)^\top}{\sqrt{2}} & \cdots & \frac{\mathbf{c}_2(k-1)^\top}{\sqrt{2}} & & 0 \\ \boldsymbol{H}_1^I(0) & \cdots & \boldsymbol{H}_1^I(k-1) & & 0 \\ & \ddots & & \ddots & \\ 0 & & \boldsymbol{H}_1^R(0) & \cdots & \boldsymbol{H}_1^R(k-1) \\ 0 & & \frac{\mathbf{c}_2(0)^\top}{\sqrt{2}} & \cdots & \frac{\mathbf{c}_2(k-1)^\top}{\sqrt{2}} \\ 0 & & \boldsymbol{H}_1^I(0) & \cdots & \boldsymbol{H}_1^I(k-1) \end{pmatrix} \in \mathbb{R}^{pM\times(k+p_1+p_2)N}.$$

c) Conclusion: In both even and odd options, we solve a linear system of the same size as the one of Section III-B, but with real coefficients in this case. More precisely, with the introduced notations, we have

$$\mathcal{H}_s\widetilde{\mathcal{H}}_s = \mathcal{U}_s = \frac{1}{2}\left[\mathbf{0}_{N,p_1N}, \boldsymbol{I}_N, \mathbf{0}_{N,(p_2+k-1)N}\right]^\top.$$

The system is then solved, in the same way as in Section III-B. For increasing values of p (starting with $p=1$), for each couple $(p_1,p_2)\in\mathbb{N}^2$ such that $p=p_1+p_2+1$ we try to invert the generated system through a Moore-Penrose pseudoinversion.

IV. Optimization

A. Dimension Reduction

1) General Case: Before addressing the issue of optimization in itself, let us rewrite the linear system expressing the PR property. The analysis FB is still supposed invertible. Let r be the rank of the matrix $\mathcal{H}\in\mathbb{C}^{(k+p_1+p_2)N\times pM}$. We assumed that $r<Mp$ (with $p=p_1+p_2+1$). Performing a singular value decomposition [47] (SVD) on this matrix yields $\mathcal{H}=\mathcal{U}_0\Sigma_0\mathcal{V}_0^*$, where $\Sigma_0\in\mathbb{C}^{r\times r}$ is an invertible diagonal matrix, $\mathcal{U}_0\in\mathbb{C}^{N(k+p-1)\times r}$ and $\mathcal{V}_0\in\mathbb{C}^{Mp\times r}$ are semi-unitary matrices (i.e., $\mathcal{U}_0^*\mathcal{U}_0=\boldsymbol{I}_r$ and $\mathcal{V}_0^*\mathcal{V}_0=\boldsymbol{I}_r$). Therefore, there exists $\mathcal{U}_1\in\mathbb{C}^{N(k+p-1)\times(N(k+p-1)-r)}$ and $\mathcal{V}_1\in\mathbb{C}^{Mp\times(Mp-r)}$ such that $[\mathcal{U}_0,\ \mathcal{U}_1]$ and $[\mathcal{V}_0,\ \mathcal{V}_1]$ are unitary matrices. When an inverse polyphase transfer matrix exists, a particular solution to (7) is $\widetilde{\mathcal{H}}^0=\mathcal{H}^\sharp\mathcal{U}$, where $\mathcal{H}^\sharp=\mathcal{V}_0\Sigma_0^{-1}\mathcal{U}_0^*$ is the pseudoinverse matrix of $\mathcal{H}$. Equation (7) is then equivalent to $\mathcal{U}_0\Sigma_0\mathcal{V}_0^*(\widetilde{\mathcal{H}}-\widetilde{\mathcal{H}}^0)=\mathbf{0}_{N(k+p-1)\times N}$. Since $\mathcal{U}_0^*\mathcal{U}_0=\boldsymbol{I}_r$ and Σ_0 is invertible, we get: $\mathcal{V}_0^*(\widetilde{\mathcal{H}}-\widetilde{\mathcal{H}}^0)=\mathbf{0}_{r\times N}$. In other words, the columns of $\widetilde{\mathcal{H}}-\widetilde{\mathcal{H}}^0$ belong to $\mathrm{Ker}(\mathcal{V}_0^*)$, the null space of $\mathcal{V}_0^*$. Moreover, it can be easily seen that $\mathrm{Ker}(\mathcal{V}_0^*)$ is equal to $\mathrm{Im}(\mathcal{V}_1)$. We then obtain the following affine form for $\mathcal{H}$:

$$\widetilde{\mathcal{H}} = \mathcal{V}_1\mathcal{C} + \widetilde{\mathcal{H}}^0 \quad (14)$$

where $\mathcal{C}\in\mathbb{C}^{(Mp-r)\times N}$.

The construction of a synthesis FB thus amounts to the choice of $\mathcal{C}$. If $\mathcal{C}=\mathbf{0}_{(Mp-r)\times N}$, then the obtained synthesis FB is the PI FB. This expression can be further rewritten into a more convenient form for optimization purposes. First, we define the matrices $(\boldsymbol{V}_j)_{j\in\{0,\ldots,M-1\}}$ by: for all $\ell\in\{-p_1,\ldots,p_2\}$ and $n\in\{0,\ldots,Mp-r-1\}$, $(\boldsymbol{V}_j)_{\ell+p_1,n}=\mathcal{V}_1((\ell+p_1)M+j,n)$, with $\mathcal{V}_1=[\mathcal{V}_1(s,n)]_{0\le s<Mp,0\le n<Mp-r}$. According to (14) and (8), we can write for all $\ell\in\{-p_1,\ldots,p_2\}$, $i\in\{0,\ldots,N-1\}$ and $j\in\{0,\ldots,M-1\}$

$$\widetilde{H}_{i,j}(\ell) = \sum_{n=0}^{Mp-r-1}(\boldsymbol{V}_j)_{\ell+p_1,n}\mathcal{C}(n,i) + \widetilde{H}_{i,j}^0(\ell)$$

where $(\widetilde{H}_{i,j}(\ell))_{-p_1\le\ell\le p_2}$ represent the impulse responses of the synthesis FB, $(\widetilde{H}_{i,j}^0(\ell))_{-p_1\le\ell\le p_2}$ correspond to the PI solution and $\mathcal{C}=[\mathcal{C}(n,i)]_{0\le n<Mp-r,0\le i<N}$. For all $j\in\{0,\ldots,M-1\}$, we introduce the matrices $\widetilde{\boldsymbol{H}}_j^0$ defined by: $(\widetilde{\boldsymbol{H}}_j^0)_{\ell+p_1,i}=\widetilde{H}_{i,j}^0(\ell)$ for all $\ell\in\{-p_1,\ldots,p_2\}$ and $i\in\{0,\ldots,N-1\}$. We, thus, obtain

$$\widetilde{H}_{i,j}(\ell) = \left(\boldsymbol{V}_j\mathcal{C} + \widetilde{\boldsymbol{H}}_j^0\right)_{\ell+p_1,i}. \quad (15)$$

This equation is used in Section IV-B-1 to simplify the optimization problem raised by the design of the synthesis FB.

The above expressions are given in the complex case, but they naturally remain valid in the real case. This will be illustrated by the first example of Section V-B-3-a.

2) Symmetric Case: In this section, we adapt the results of the previous section to the HS FB case. The notations used here are similar to those introduced in Section III-C-2. It is worth noticing that we can calculate the matrix $\widetilde{\mathcal{H}}$ directly from $\widetilde{\mathcal{H}_s}$, as defined in Section III-C-2 when M is either even or odd, in the following way:

$$\widetilde{\mathcal{H}} = \boldsymbol{P}_{\mathrm{rc}}\widetilde{\mathcal{H}_s} \quad (16)$$

where the matrix $\boldsymbol{P}_{\mathrm{rc}}\in\mathbb{C}^{pM\times pM}$ is the block diagonal matrix built with the block:

$$\begin{pmatrix} \boldsymbol{I}_{M'} & -\imath\boldsymbol{I}_{M'} \\ \boldsymbol{J}_{M'} & \imath\boldsymbol{J}_{M'} \end{pmatrix}$$

if $M=2M'$ (even case, as seen in Section III-C-2-a) and

$$\begin{pmatrix} \boldsymbol{I}_{M'} & 0 & -\imath\boldsymbol{I}_{M'} \\ 0 & \sqrt{2} & 0 \\ \boldsymbol{J}_{M'} & 0 & \imath\boldsymbol{J}_{M'} \end{pmatrix}$$

if $M=2M'+1$ (odd case, as seen in Section III-C-2-b). By applying once again an SVD on $\mathcal{H}_s$, and by following the same steps as in Section IV-A-1, we end up with an equation similar to (14):

$$\widetilde{\mathcal{H}_s} = \mathcal{V}_1\mathcal{C} + \widetilde{\mathcal{H}_s}^0. \quad (17)$$

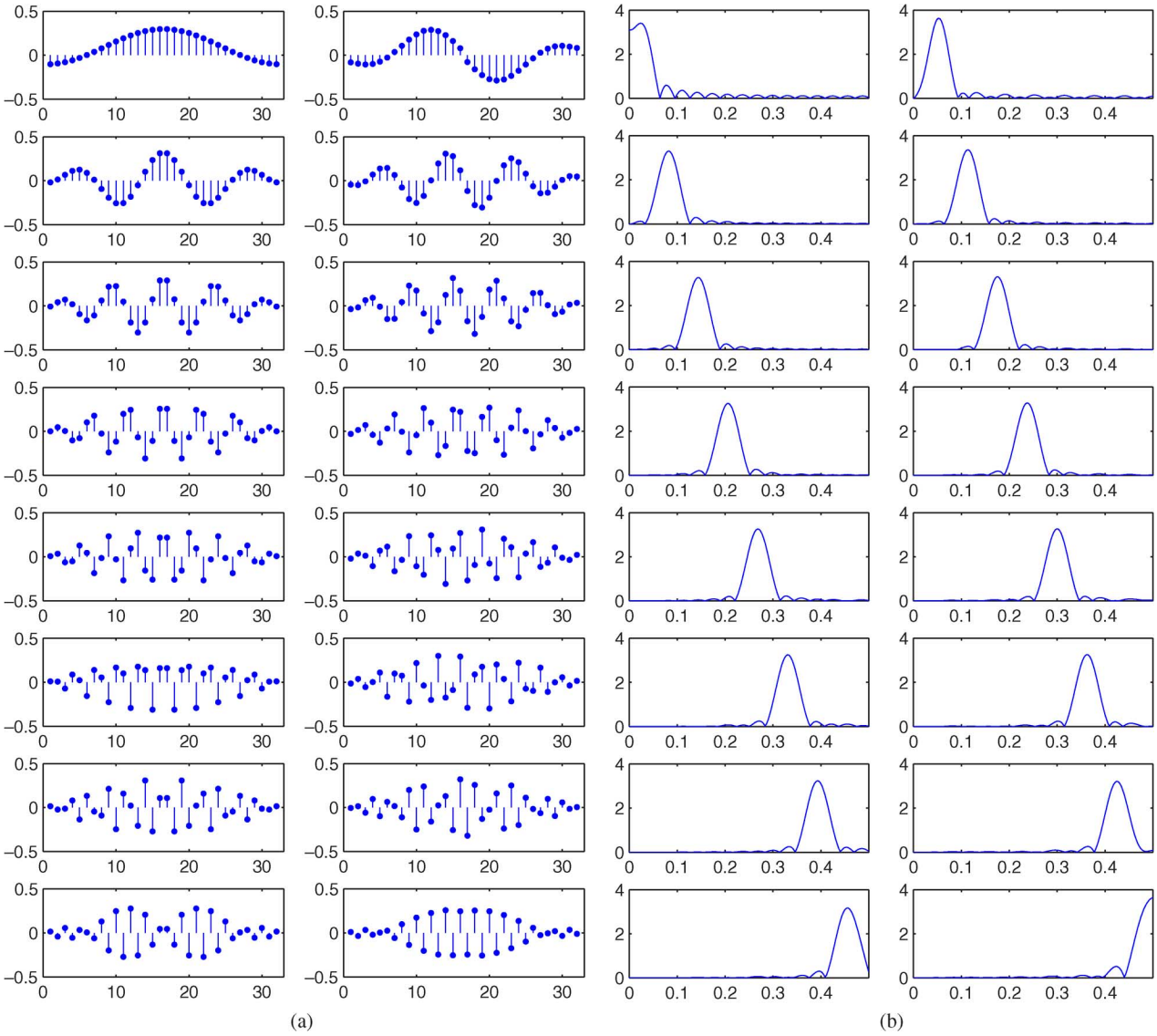

Fig. 2. (a) Impulse. (b) Frequency responses of a GenLOT analysis FB.

Note that, according to the properties of the SVD, the matrix $\mathcal{C}$ is now real-valued. By noticing that $\widetilde{\mathcal{H}}^0 = \boldsymbol{P}_{\mathrm{rc}}\widetilde{\mathcal{H}_s}^0$ and setting $\mathcal{W}_1 = \boldsymbol{P}_{\mathrm{rc}}\mathcal{V}_1$, we finally obtain

$$\widetilde{\mathcal{H}} = \mathcal{W}_1\mathcal{C} + \widetilde{\mathcal{H}}^0. \tag{18}$$

We next define the matrices $(\boldsymbol{W}_j)_{0\le j\le M-1}$: for all $\ell \in \{-p_1,\ldots,p_2\}$ and $n \in \{0,\ldots,Mp-r-1\}$: $(\boldsymbol{W}_j)_{\ell+p_1,n} = \mathcal{W}_1((\ell+p_1)M+j,n)$. Using (18) as in Section IV-A-1, we get

$$\widetilde{H}_{i,j}(\ell) = \left(\boldsymbol{W}_j\mathcal{C} + \widetilde{\boldsymbol{H}}_j^0\right)_{\ell+p_1,i}. \tag{19}$$

B. Optimal Solution

1) General Form for the Cost Functions: Depending on the desired properties for the synthesis FB, several cost functions can be employed. We first propose a generic cost function formulation and then provide practical examples based on the filter time or frequency spread, respectively.

Our goal is to optimize the filter shape given by the coefficients $\widetilde{h}$ of the synthesis FB, subject to the perfect reconstruction property. According to the results in Section IV-A, it is possible to represent the coefficients in the general case by using (15). The optimization favorably takes place in the reduced dimension space the matrix $\mathcal{C}$ belongs to (compared with the dimension of the space of the coefficients of $\widetilde{h}$), thus allowing us to reformulate the optimization under a perfect reconstruction constraint as an unconstrained problem. In this context, the generic cost function form we consider is

$$J(\widetilde{h}) = \widetilde{J}(\mathcal{C}) = \sum_{j=0}^{M-1} \frac{\left\|\boldsymbol{V}_j\mathcal{C} + \widetilde{\boldsymbol{H}}_j^0\right\|_{K_j}^2}{\left\|\boldsymbol{V}_j\mathcal{C} + \widetilde{\boldsymbol{H}}_j^0\right\|_{\Lambda}^2}.$$

Here, the following notation has been employed:

$$\forall \boldsymbol{A} \in \mathbb{C}^{N\times p}, \quad \|\boldsymbol{A}\|_K^2 = \sum_{(i,i',\ell,\ell')} \boldsymbol{A}_{i,\ell}\overline{\boldsymbol{A}_{i',\ell'}} K(i,i',\ell,\ell')$$

where K and Λ are $(N\times N\times p\times p)$ kernels. Moreover, we assume here that $\|\boldsymbol{A}\|_K$ represents a seminorm over $\mathbb{C}^{N\times p}$ and it is thus real nonnegative. Let $\boldsymbol{K}'$ be the matrice defined by $\boldsymbol{K}'_{i+\ell N,i'+\ell' N} = K(i,i',\ell,\ell')$ for all $(\ell,\ell') \in \{0,\dots,p-1\}^2$ and $(i,i') \in \{0,\dots,N-1\}^2$. Without loss of generality, this matrix can be taken positive semidefinite, which implies that $\boldsymbol{K}'_{i+\ell N,i'+\ell' N} = \overline{\boldsymbol{K}_{i'+\ell' N,i+\ell N}}'$ and, thus, $K(i,i',\ell,\ell') = \overline{K(i',i,\ell',\ell)}$. We deduce the following expression:

$$\begin{aligned}\|\boldsymbol{A}\|_K^2 &= \sum_{(i,i',\ell,\ell')} \boldsymbol{A}_{i,\ell}\overline{\boldsymbol{A}_{i',\ell'}} K(i,i',\ell,\ell') \\ &= \sum_{(i,i',\ell,\ell')} \boldsymbol{A}_{i,\ell}\overline{\boldsymbol{A}_{i',\ell'} K(i',i,\ell',\ell)}.\end{aligned}$$

This relation will be used to simplify some equations in Section IV-C and Appendix C. We finally notice that $\boldsymbol{K}'$ is a positive definite Hermitian matrix if and only if $\|.\|_K$ is a norm.

2) Impulse Responses Optimization: A first objective is to obtain impulse responses $(\widetilde{h}_j)_{0\le j<M}$ for the synthesis filters well-localized, around some time-indices $(\overline{m}_j)_{0\le j<M}$. We now explain the link between the cost function form introduced in the previous section and the previously described dimension reduction to further simplify the problem.

The considered cost function is the following:

$$J_{\mathrm{t}}(\widetilde{h}) = \sum_{j=0}^{M-1} \omega_{\mathrm{t},j} \frac{\sum_m |m-\overline{m}_j|^\alpha |\widetilde{h}_j(m)|^2}{\sum_m |\widetilde{h}_j(m)|^2}$$

with $\alpha \in \mathbb{R}_+^*$ and weights $(\omega_{\mathrm{t},j})_{0\le j<M} \in (\mathbb{R}_+)^M$ such that $\sum_{j=1}^{M-1}\omega_{\mathrm{t},j} = 1$. If $\alpha = 2$ and $\overline{m}_j = \sum_m m|\widetilde{h}_j(m)|^2 / \sum_m |\widetilde{h}_j(m)|^2$, then $J_{\mathrm{t}}(\widetilde{h})$ represents a weighted sum of the standard temporal dispersions measuring the time localization of a filter $\widetilde{h}_j$ [48]. Combined with (6), we get

$$\begin{aligned}&J_{\mathrm{t}}(\widetilde{h}) \\ &= \sum_{j=0}^{M-1} \omega_{\mathrm{t},j} \frac{\sum_{\ell=-p_1}^{p_2}\sum_{i=0}^{N-1} |\ell N - i - \overline{m}_j|^\alpha \left|\widetilde{h}_j(\ell N - i)\right|^2}{\sum_{\ell=-p_1}^{p_2}\sum_{i=0}^{N-1} \left|\widetilde{h}_j(\ell N - i)\right|^2} \\ &= \sum_{j=0}^{M-1} \omega_{\mathrm{t},j} \frac{\sum_{\ell=-p_1}^{p_2}\sum_{i=0}^{N-1} |\ell N - i - \overline{m}_j|^\alpha \left|\widetilde{H}_{i,j}(\ell)\right|^2}{\sum_{\ell=-p_1}^{p_2}\sum_{i=0}^{N-1} \left|\widetilde{H}_{i,j}(\ell)\right|^2}.\end{aligned}$$

We now introduce the kernels K_j^{t} and Λ defined by

$$\begin{aligned}K_j^{\mathrm{t}}(i,i',\ell+p_1,\ell'+p_1) &= \omega_{\mathrm{t},j}\,|\ell N - i - \overline{m}_j|^\alpha\,\delta_{i-i'}\delta_{\ell-\ell'} \\ \Lambda(i,i',\ell+p_1,\ell'+p_1) &= \delta_{i-i'}\delta_{\ell-\ell'},\end{aligned} \tag{20}$$

for all $j \in \{0,\dots,M-1\}$, $(\ell,\ell') \in \{-p_1,\dots,p_2\}^2$ and $(i,i') \in \{0,\dots,N-1\}^2$. Using (15) we write

$$\sum_{\ell=-p_1}^{p_2}\sum_{i=0}^{N-1} \left|\widetilde{H}_{i,j}(\ell)\right|^2 = \left\|\boldsymbol{V}_j\mathcal{C} + \widetilde{\boldsymbol{H}}_j^0\right\|_\Lambda^2$$

and

$$\omega_{\mathrm{t},j}\sum_{\ell=-p_1}^{p_2}\sum_{i=0}^{N-1}(\ell N - i - \overline{m}_j)^2 \left|\widetilde{H}_{i,j}(\ell)\right|^2 = \left\|\boldsymbol{V}_j\mathcal{C} + \widetilde{\boldsymbol{H}}_j^0\right\|_{K_j^{\mathrm{t}}}^2.$$

Here, $\|.\|_\Lambda$ reduces to the Frobenius norm. Finally, we deduce that

$$J_{\mathrm{t}}(\widetilde{h}) = \sum_{j=0}^{M-1} \frac{\left\|\boldsymbol{V}_j\mathcal{C} + \widetilde{\boldsymbol{H}}_j^0\right\|_{K_j^{\mathrm{t}}}^2}{\left\|\boldsymbol{V}_j\mathcal{C} + \widetilde{\boldsymbol{H}}_j^0\right\|_\Lambda^2} = \widetilde{J}_{\mathrm{t}}(\mathcal{C}).$$

The constrained minimization of J_{t} is then reexpressed as the unconstrained minimization of $\widetilde{J}_{\mathrm{t}}$.

3) Frequency Response Optimization: We proceed similarly to the previous section, for a different cost function $J_{\mathrm{f}}(\widetilde{h})$. Our goal, dual to that in the previous section, is now to regularize the frequency responses of the synthesis FB by concentrating the frequency response of each filter $\widetilde{h}_j$ around some frequency f_j. This is achieved by minimizing

$$J_{\mathrm{f}}(\widetilde{h}) = \sum_{j=0}^{M-1} \omega_{\mathrm{f},j} \frac{\int_{-1/2+f_j}^{1/2+f_j} |\nu - f_j|^\alpha \left|\widetilde{h}_j[\nu]\right|^2 d\nu}{\int_{-1/2+f_j}^{1/2+f_j} \left|\widetilde{h}_j[\nu]\right|^2 d\nu} \tag{21}$$

where $\alpha \in \mathbb{R}_+^*$, $(\omega_{\mathrm{f},j})_{0\le j<M} \in (\mathbb{R}_+^*)^M$ with $\sum_{j=0}^{M-1}\omega_{\mathrm{f},j} = 1$ and, $\widetilde{h}_j[.]$ is the frequency response of the jth synthesis filter, defined as

$$\forall \nu \in [-1/2, 1/2[, \quad \widetilde{h}_j[\nu] = \sum_{\ell=-p_1}^{p_2}\sum_{i=0}^{N-1} \widetilde{H}_{i,j}(\ell) e^{-2\imath\pi(N\ell-i)\nu}.$$

When $f_j = (\int_{-1/2}^{1/2} \nu|\widetilde{h}_j[\nu]|^2 d\nu / \int_{-1/2}^{1/2} |\widetilde{h}_j[\nu]|^2 d\nu)$, the cost function $J_{\mathrm{f}}(\widetilde{h})$ represents a classical weighted frequency dispersion measure for the synthesis filters. We then define the kernel

$$\begin{aligned}&K_j^{\mathrm{f}}(i,i',\ell+p_1,\ell'+p_1) \\ &\quad= \omega_{\mathrm{f},j}\int_{-1/2+f_j}^{1/2+f_j} |\nu - f_j|^\alpha e^{-2\imath\pi\left(N(\ell-\ell')-(i-i')\right)\nu} d\nu \\ &\quad= \omega_{\mathrm{f},j}\int_{-1/2}^{1/2} |\nu|^\alpha e^{-2\imath\pi\left(N(\ell-\ell')-(i-i')\right)(\nu+f_j)} d\nu\end{aligned} \tag{22}$$

with $(i,i',\ell,\ell') \in \{0,\dots,N-1\}^2 \times \{-p_1,\dots,p_2\}^2$.

Remark 2: The examples provided in Section V-B-3 are obtained with $\alpha = 2$. In this case, the explicit expression of the

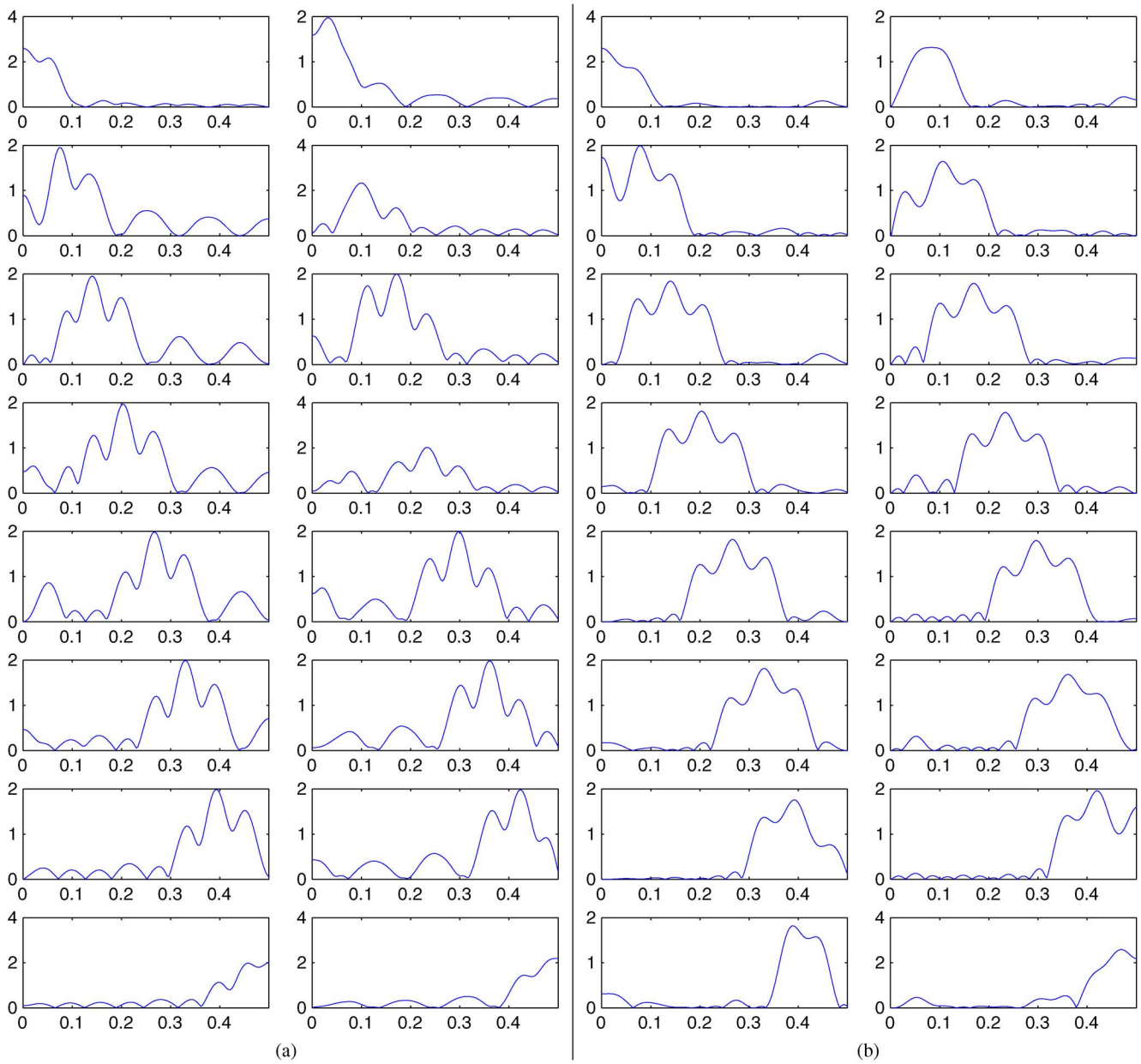

Fig. 3. First example (with the GenLOT FB of Section V-A-1): frequency response of the synthesis FB obtained (a) through the pseudoinverse method. (b) After optimization with cost function $\widetilde{J}_{\mathrm{t}}$.

kernel becomes (see the equation at the bottom of the page), with $(i,i',\ell,\ell') \in \{0,\ldots,N-1\}^2 \times \{-p_1,\ldots,p_2\}^2$.

Combining these notations and (15), we have

$$\omega_{\mathrm{f},j} \int_{-1/2+f_j}^{1/2+f_j} |\nu - f_j|^{\alpha} \left|\widetilde{h}_j[\nu]\right|^2 d\nu = \left\| \boldsymbol{V}_j \mathcal{C} + \widetilde{\boldsymbol{H}}_j^0 \right\|_{K_j^{\mathrm{f}}}^2 .$$

Invoking Plancherel's theorem and the kernel Λ defined in Section IV-B-2, we obtain

$$\int_{-1/2+f_j}^{1/2+f_j} \left|\widetilde{h}_j[\nu]\right|^2 d\nu = \sum_{\ell=-p_1}^{p_2} \sum_{i=0}^{N-1} \left|\widetilde{H}_{i,j}(\ell)\right|^2 = \left\| \boldsymbol{V}_j \mathcal{C} + \widetilde{\boldsymbol{H}}_j^0 \right\|_{\Lambda}^2 .$$

Finally, substituting these expressions in (21) yields

$$K_j^{\mathrm{f}}(i,i',\ell+p_1,\ell'+p_1) = \begin{cases} \frac{\omega_{\mathrm{f},j}}{12}, & \text{if } i=i' \text{ and } \ell=\ell' \\ \frac{\omega_{\mathrm{f},j}(-1)^{N(\ell-\ell')-(i-i')} e^{-2\imath\pi(N(\ell-\ell')-(i-i'))f_j}}{2\pi^2(N(\ell-\ell')-(i-i'))^2}, & \text{otherwise} \end{cases}$$

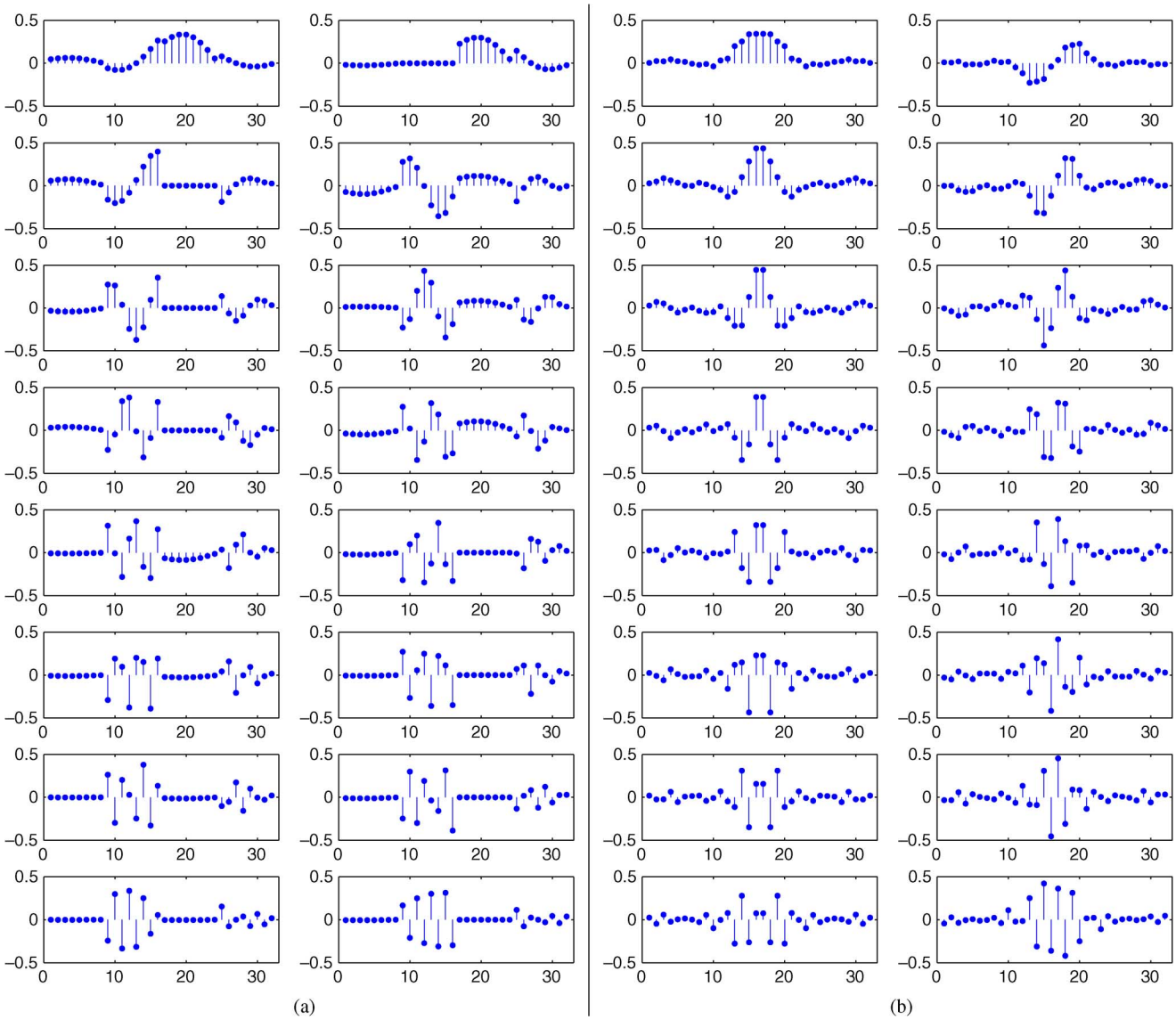

Fig. 4. First example: impulse response of the synthesis FB obtained (a) through the pseudoinverse method. (b) After optimization with cost function $\widetilde{J}_{\mathrm{t}}$.

$$J_{\mathrm{f}}(\widetilde{h}) = \sum_{j=0}^{M-1} \frac{\left\| \boldsymbol{V}_j \mathcal{C} + \widetilde{\boldsymbol{H}}_j^0 \right\|_{K_j^{\mathrm{f}}}^2}{\left\| \boldsymbol{V}_j \mathcal{C} + \widetilde{\boldsymbol{H}}_j^0 \right\|_{\Lambda}^2} = \widetilde{J}_{\mathrm{f}}(\mathcal{C}).$$

Once again, the constrained optimization problem has been reformulated as an unconstrained one.

C. Gradient Optimization

The constrained optimization problem being turned into an unconstrained minimization, we now provide more details about the minimization algorithm we employ. In this paper, we have used a simple gradient algorithm with an adaptive step μ_n. The algorithm can be summarized as follows:

① Initialization: $\mathcal{C}_0 = \mathbf{0}$, $n = 0$.

② $\mu_n = 1$

③ Computation of $\boldsymbol{D}_n = \nabla \widetilde{J}(\mathcal{C}_n)$.

④ While $\widetilde{J}(\mathcal{C}_n - \mu_n \boldsymbol{D}_n) \geq \widetilde{J}(\mathcal{C}_n)$, set $\mu_n \leftarrow (1/(1/\mu_n) + 1)$.

⑤ $\mathcal{C}_{n+1} = \mathcal{C}_n - \mu_n \boldsymbol{D}_n$.

⑥ If $\|\mathcal{C}_{n+1} - \mathcal{C}_n\| > \epsilon$ then increment n and go to step ② .

The step-size μ_n used here remains large as long as the algorithm is getting closer to a local minimum (in other words, as long as $\widetilde{J}(\mathcal{C}_{n+1}) < \widetilde{J}(\mathcal{C}_n)$). It is only adapted (reduced) to prevent the criterion from increasing. The initialization with $\mathcal{C}_0 = \mathbf{0}$ entails that we consider the pseudoinverse synthesis FB as the starting point for the algorithm. In practice, ϵ was set to 10^{-13}.

Other step selection strategies exist: constant or optimal steps, steps satisfying Wolfe or Armijo conditions [49], [50]. The method used in this work is easy to implement and is well suited to the different cost functions we have considered, while keeping a reasonable complexity.

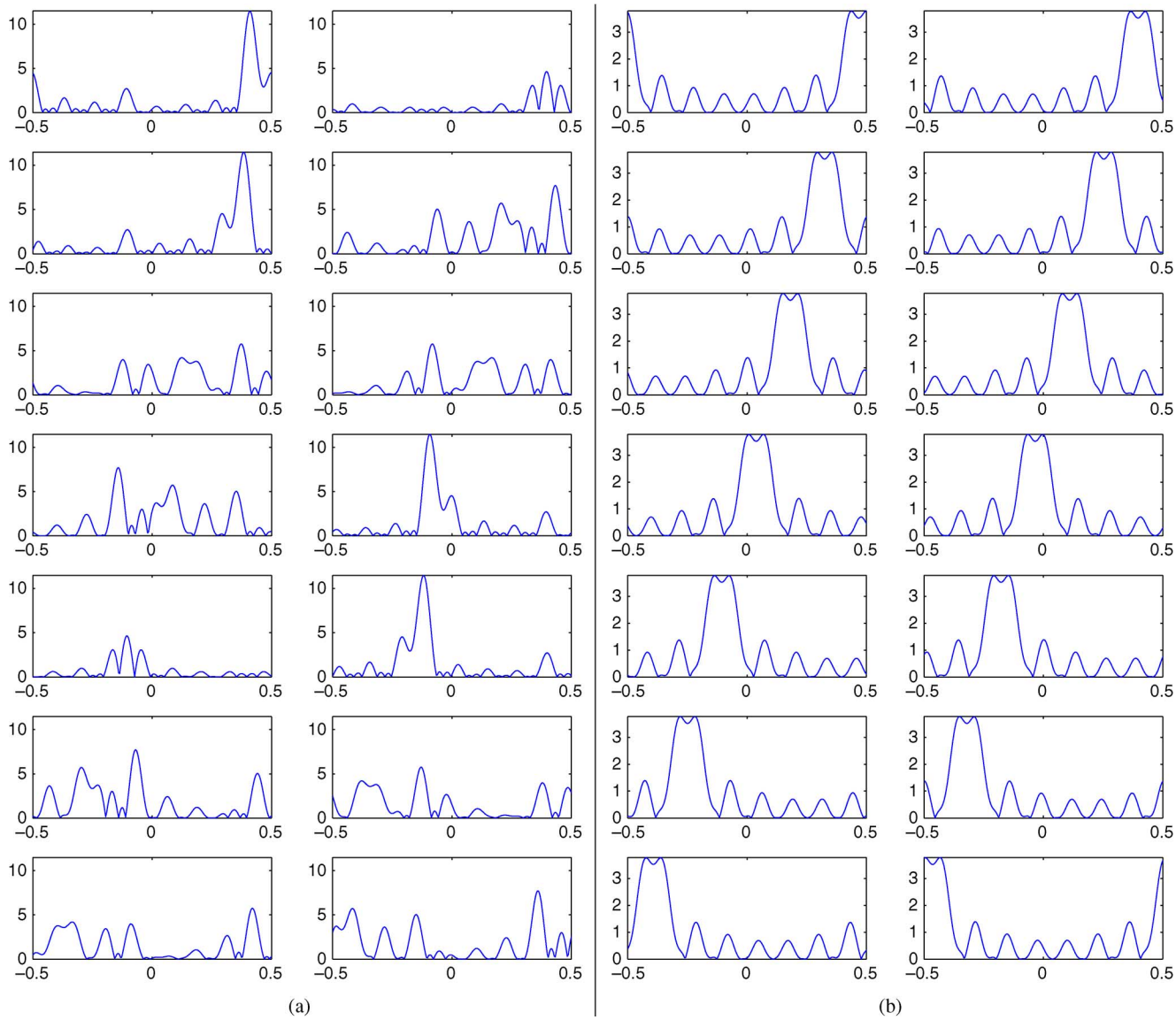

Fig. 5. Second example (in the MCLT case with window h_{a_1}): frequency responses of synthesis filters (a) before and (b) after optimization with the cost function $\widetilde{J}_{\mathsf{f}}$.

As the cost functions considered in this work are not convex, there is no theoretical guarantee that the algorithm converges to a global minimum. Yet, as is shown in Section V, initializing this method with the PI synthesis FB provides quite good results and extensive simulations have confirmed this good behavior.

The expression of the gradient for the general cost function is given in Appendix A and is next applied to $\widetilde{J}_{\mathsf{t}}$ and $\widetilde{J}_{\mathsf{f}}$ in Appendix B.

D. Optimal Solution in the Symmetric Case

1) Cost Functions: Using the same notations as in Section IV-B, in the HS case, the following form of the cost function is found:

$$J_{\mathsf{s}}(\widetilde{h}) = \widetilde{J}_{\mathsf{s}}(\mathcal{C}) = \sum_{j=0}^{M-1} \frac{\left\| \boldsymbol{W}_j \mathcal{C} + \widetilde{\boldsymbol{H}}_j^0 \right\|_{K_j}^2}{\left\| \boldsymbol{W}_j \mathcal{C} + \widetilde{\boldsymbol{H}}_j^0 \right\|_{\Lambda}^2}.$$

As in the general case, (19) has been used to transform the constrained optimization problem on $\widetilde{h}$ into an unconstrained minimization problem on $\mathcal{C}$.

2) Examples of Cost Functions: Equation (19) is very similar to (15). We consequently define the cost functions in the HS case following the same approach as in Sections IV-B-2 and IV-B-3. Thus, the following functions are considered:

$$\widetilde{J}_{\mathsf{ts}}(\mathcal{C}) = \sum_{j=0}^{M-1} \frac{\left\| \boldsymbol{W}_j \mathcal{C} + \widetilde{\boldsymbol{H}}_j^0 \right\|_{K_j^{\mathrm{t}}}^2}{\left\| \boldsymbol{W}_j \mathcal{C} + \widetilde{\boldsymbol{H}}_j^0 \right\|_{\Lambda}^2}$$

to concentrate the time localization of impulse responses, and

$$\widetilde{J}_{\mathsf{fs}}(\mathcal{C}) = \sum_{j=0}^{M-1} \frac{\left\| \boldsymbol{W}_j \mathcal{C} + \widetilde{\boldsymbol{H}}_j^0 \right\|_{K_j^{\mathrm{f}}}^2}{\left\| \boldsymbol{W}_j \mathcal{C} + \widetilde{\boldsymbol{H}}_j^0 \right\|_{\Lambda}^2}$$

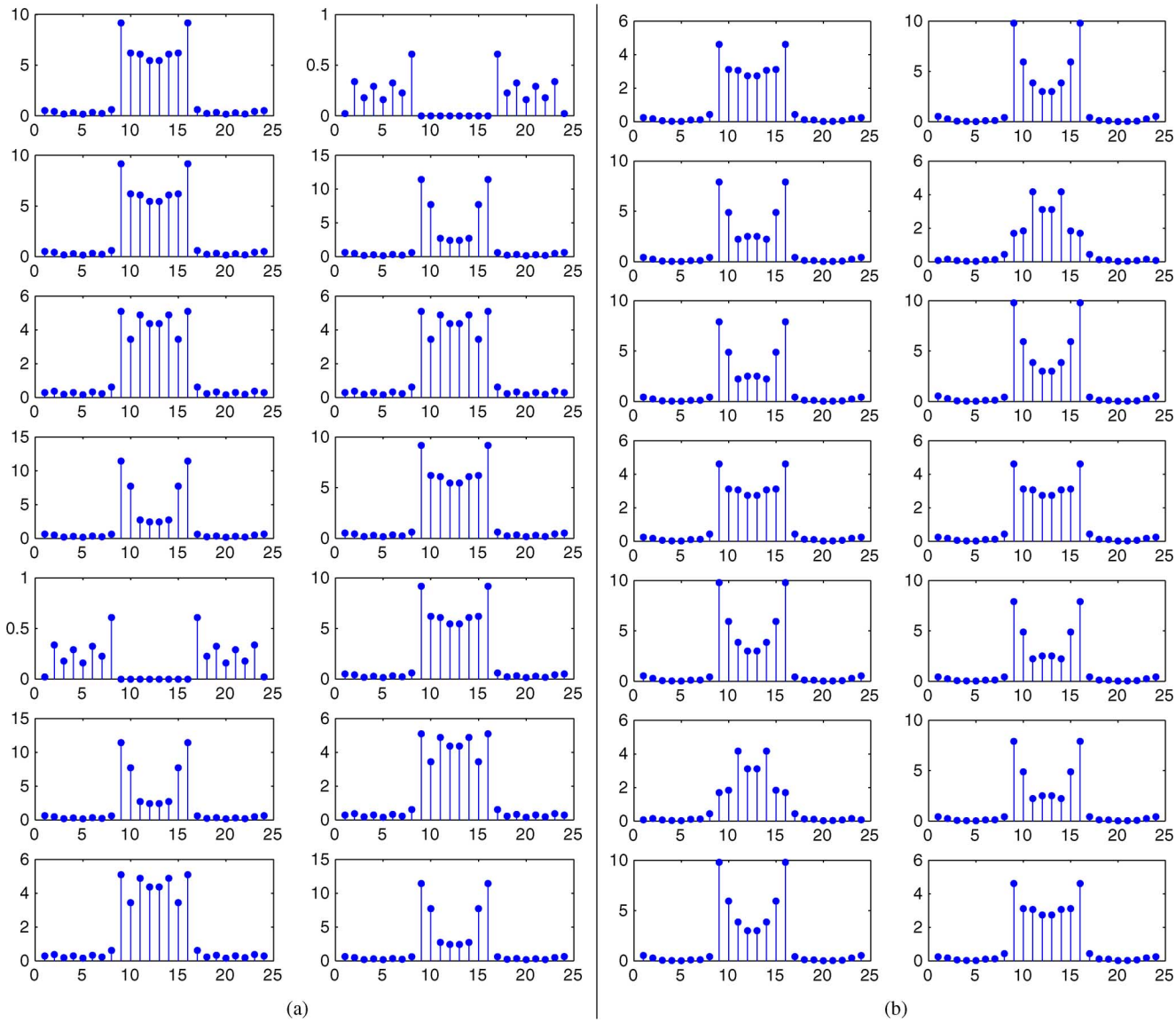

Fig. 6. Modulus of the impulse responses of the synthesis FBs (in the MCLT case with h_{a_2} window). (a) Pseudoinverse. (b) Symmetric version with the method of Section III-C-2.

TABLE I
COMPUTATION TIME TO OPTIMIZE A SYNTHESIS FB WITH DIFFERENT METHODS USING MATLAB

	$N = 4$	$N = 8$	$N = 16$
Constrained optimization (with `fmincon`)	1.2s	120s	8800s
Unconstrained optimization (with `fminunc`)	0.04s	0.7s	8s
Unconstrained optimization (gradient algorithm)	0.06s	0.6s	7s

to enhance the frequency selectivity of the filters. Their gradients are provided in Appendix C.

V. EXAMPLES

As emphasized earlier, a wide variety of filter banks and design choices can be made. In this section, we have chosen to work with three different examples exhibiting interesting properties and allowing us to show the benefits incurred in the proposed inversion and optimization methods.

A. Considered Filter Banks

1) Real Lapped Transforms: The study, developed for the general complex case, remains fully applicable to the design of real filter banks. As an illustration, we first consider real lapped transforms introduced in the middle of the 1990s under the name of *GenLOT* (generalized linear-phase lapped orthogonal transform) [51]. Those transforms generalize the discrete cosine transform (DCT) and the lapped orthogonal transform (LOT).

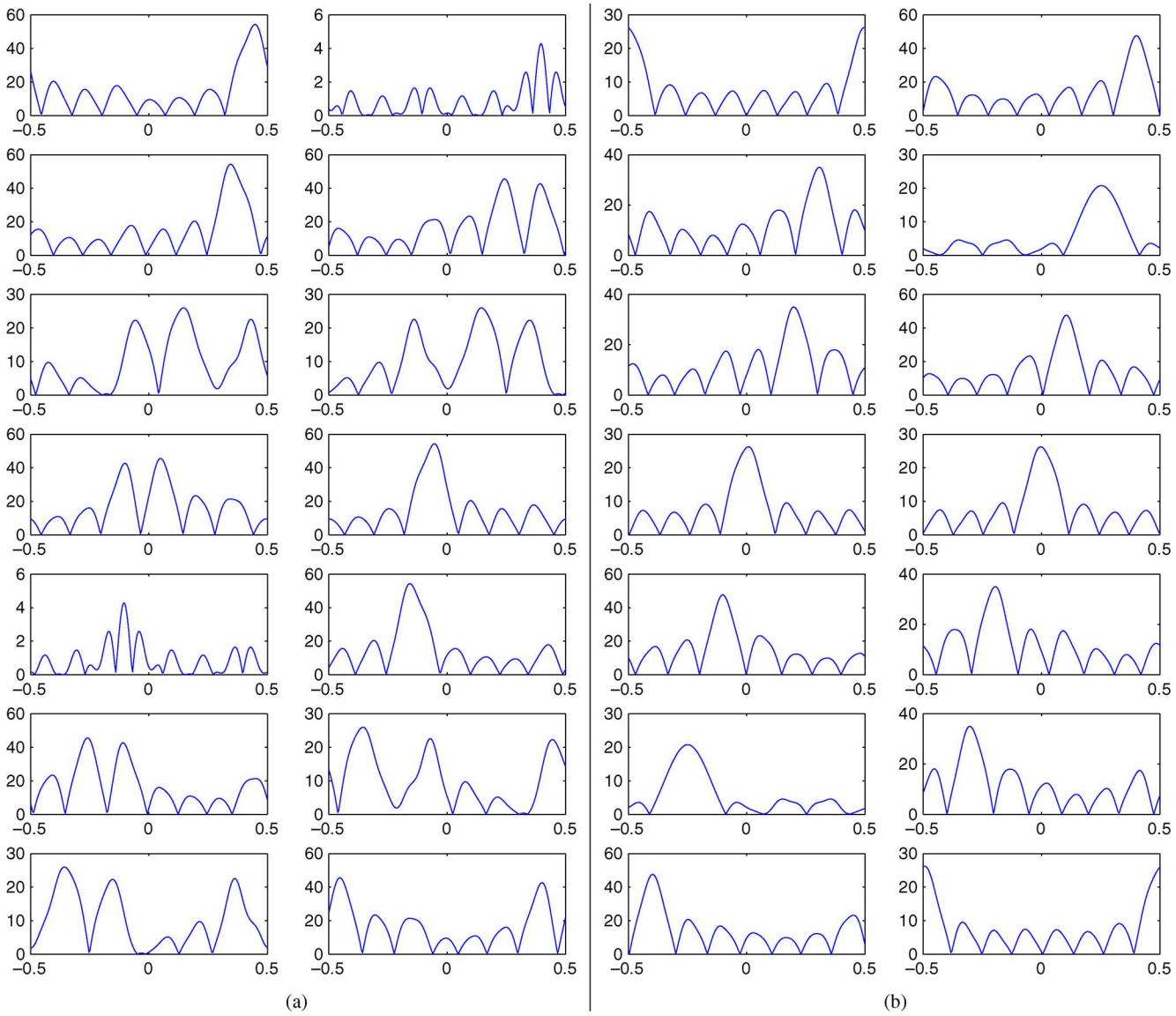

Fig. 7. Frequency responses of the synthesis FBs (in the MCLT case with h_{a_2} window): (a) pseudoinverse and (b) symmetric version with the method of Section III-C-2.

To illustrate the inversion method, we have chosen a GenLOT with $M = 16$ filters of 32 coefficients. This FB is invertible, in a nonstandard oversampled use, with parameters $N = 8$, $k = 4$ and $k' = 2$. Its impulse and frequency responses are represented in Fig. 2. This FB is real and does not satisfy the HS condition. By using the method described in Section III-B, we find $p_1 = 3$ and $p_2 = 0$ (hence, $p = 4$). The frequency and impulse responses of the synthesis FB computed with the pseudoinverse are shown on Figs. 3(a) and 4(a).

2) Modulated Complex Lapped Transform: We now consider another analysis FB based on a windowed generalized Fourier transform, corresponding to a modulated complex lapped transform (*MCLT*). This family of FB has been used by Kingsbury [4] or Malvar [7] for applications in video as well as audio processing. The analysis impulse responses are: $h_i(n) = \boldsymbol{E}(i,n)h_{\mathsf{a}}(n)$, where

$$\boldsymbol{E}(i,n) = \frac{1}{\sqrt{k'N}} e^{-\imath\left(i-\frac{k'N}{2}+\frac{1}{2}\right)\left(n-\frac{kN}{2}+\frac{1}{2}\right)\frac{2\pi}{k'N}}$$

and $(h_{\mathsf{a}}(n))_{1\le n\le kN}$ is an analysis window. In this paper, we consider two analysis windows. The first, defined by

$$\forall n\{1,\ldots,kN\}, \quad h_{\mathsf{a}_1}(n) = \sin\left(\frac{n\pi}{kN+1}\right)$$

is a standard sine window, employed for example in [4] and [7]. The second $(h_{\mathsf{a}_2}(n))_{1\le n\le kN}$, corresponds to a zero-phase low-pass filter with cutoff frequency $2\pi/(kN)$, built from a Kaiser window. This window, with better tapering than h_{a_1}, was used for instance in [32]. It is interesting to note that this analysis FB family, with both analysis windows, satisfies Condition (11). In other words, it can be used to illustrate our approach in the HS case. The method from Section III-A was employed to verify the invertibility on this FB, with both analysis windows and parameters $N = 8$, $k = 3$ and $k' = 7/4$. We then compute a first synthesis FB with the PI method of Section III-B. For the analysis FB with h_{a_1} window, the minimal parameters $p_1 = 2$ and $p_2 = 0$ were obtained. The frequency response of this synthesis FB is represented in Fig. 5(a). In the h_{a_2} case, the minimal

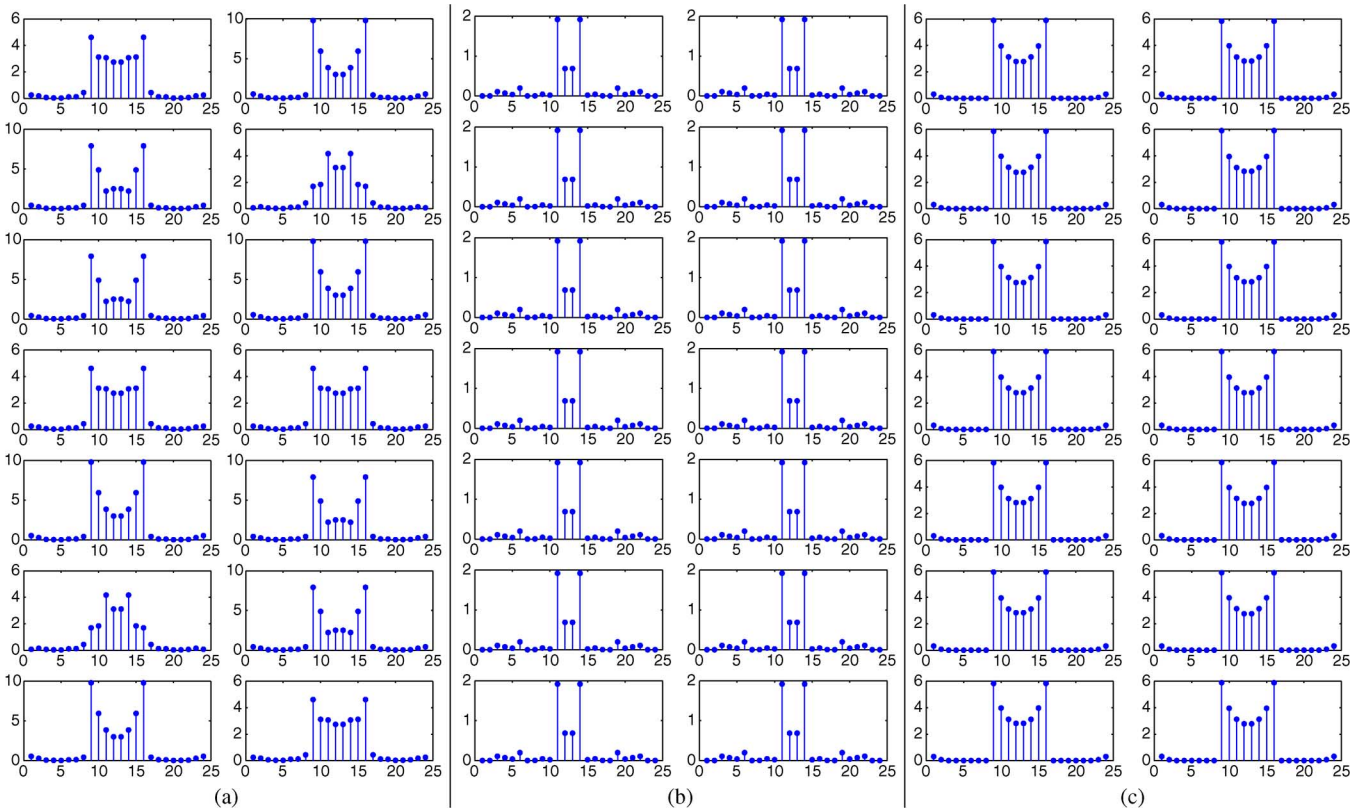

Fig. 8. Third example (in the MCLT case with window h_{a_2}): modulus of the impulse responses of synthesis filters (a) before and after optimization (b) with the cost function $\widetilde{J}_{\mathsf{ts}}$ and (c) with $\widetilde{J}_{\mathsf{fs}}$.

TABLE II
FREQUENCY DISPERSION OF THE SYNTHESIS FILTERS OPTIMIZED WITH COST FUNCTION $\widetilde{J}_{\mathsf{f}}$

Filter	Freq. disp.	Filter	Freq. disp.
$\widetilde{h}_0$	0.0290	$\widetilde{h}_0^{opt}$	0.0111
$\widetilde{h}_1$	0.0851	$\widetilde{h}_1^{opt}$	0.0110
$\widetilde{h}_2$	0.0569	$\widetilde{h}_2^{opt}$	0.0109
$\widetilde{h}_3$	0.0606	$\widetilde{h}_3^{opt}$	0.0112
$\widetilde{h}_4$	0.0658	$\widetilde{h}_4^{opt}$	0.0110
$\widetilde{h}_5$	0.0596	$\widetilde{h}_5^{opt}$	0.0109
$\widetilde{h}_6$	0.0363	$\widetilde{h}_6^{opt}$	0.0111
$\widetilde{h}_7$	0.0156	$\widetilde{h}_7^{opt}$	0.0111
$\widetilde{h}_8$	0.0411	$\widetilde{h}_8^{opt}$	0.0109
$\widetilde{h}_9$	0.0231	$\widetilde{h}_9^{opt}$	0.0110
$\widetilde{h}_{10}$	0.0508	$\widetilde{h}_{10}^{opt}$	0.0112
$\widetilde{h}_{11}$	0.0499	$\widetilde{h}_{11}^{opt}$	0.0110
$\widetilde{h}_{12}$	0.0574	$\widetilde{h}_{12}^{opt}$	0.0109
$\widetilde{h}_{13}$	0.0521	$\widetilde{h}_{13}^{opt}$	0.0111
Sum	0.6833		0.1544

parameters $p_1 = 2$ and $p_2 = 0$ were, once again, found when applying the method of Section III-B. An HS synthesis FB is then derived from this filter bank using the method of Section III-C-2 to directly build an HS synthesis FB. The frequency and impulse responses of the resulting synthesis FBs, in the h_{a_2} case, are shown in Figs. 6 and 7, respectively. Fig. 6(a) shows that synthesis filters present a symmetric behavior for their coefficients (in other words, they have a linear phase) while the synthesis FB in itself is not HS. We also notice that the frequency selectivity or time-frequency localization of the filters obtained through the pseudoinverse methods is not satisfactory.

B. Optimization Examples

1) Kernel Parameters:

a) Temporal kernel K_j^{t}: It is defined by (20). The parameters $\overline{m}_j$ define the (temporal) positions around which the impulse responses of the jth filter should be concentrated. To obtain well tapered filters, we need to concentrate the impulse responses around the middle of the filter support. Therefore, the same parameter was used for all filters. The support of the filters being $\{-p_1N - N + 1, \ldots, p_2N\}$, we have chosen $\overline{m}_j$ as

$$\forall 0 \leq j < M, \qquad \overline{m}_j = \overline{m} = \frac{p_2N + 1 - p_1N - N}{2}.$$

In our design example, α has been set to 2.

b) Frequency kernel K_j^{f}: It is defined by (22). The parameters f_j represent the reduced frequencies around which we want to concentrate the frequency responses of the synthesis filters. More precisely, we chose f_j such that it is centered inside the bandwidth of the analysis filter h_j. The exponent α has been set to 2.

c) Weight parameters: In the proposed cost functions, the parameters $\omega_{\mathsf{t},j}$ and $\omega_{\mathsf{f},j}$ control the relative importance of the

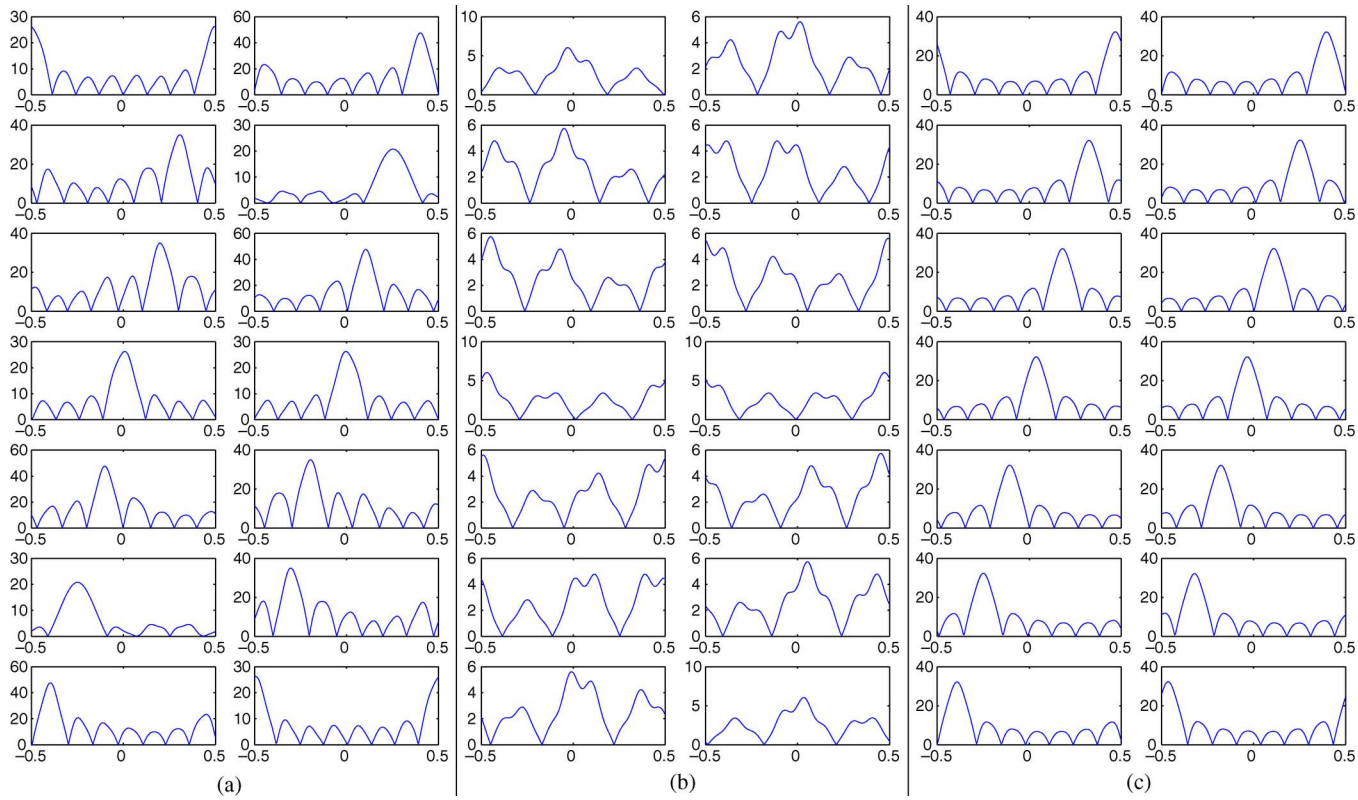

Fig. 9. Third example (in the MCLT case with window h_{a_2}): frequency responses of synthesis filters (a) before and after optimization (b) with the cost function $\widetilde{J}_{\mathsf{ts}}$ and (c) with $\widetilde{J}_{\mathsf{fs}}$.

different filters in the optimization process. For the following examples we have chosen equal weights:

$$\forall j \in \{0, \ldots, M-1\},\ \ \omega_{\mathsf{t},j} = \omega_{\mathsf{f},j} = \frac{1}{M}.$$

In other words, we aim at obtaining synthesis filters with similar behavior.

2) Computation Time: In Section IV-A, we have seen how to parameterize the system and thus how to reduce the dimension of the optimization problem. To evaluate the gain resulting from this parameterization, Matlab programs were written to compare the solutions of the constrained problem, using function `fmincon`, with the solutions of the unconstrained problem, using function `fminunc` and using the gradient method explained in Section IV-C. The two functions `fmincon` and `fminunc` were chosen as examples of optimization implementation, while the gradient procedure can be easily applied in different languages without requiring Matlab. These programs were tested with the analysis FB introduced in Section V-A-2 with the h_{a_1} window and the following parameters: overlap factor $k = 3$, redundancy $k' = 7/4$ and downsampling $N \in \{4, 8, 16\}$. The cost function used was J_{t} (as defined in Section IV-B-2). Table I shows the computation time for the different methods on a computer with 2.16 GHz Intel Core2 T7400 CPU and 2Gb of RAM.

A first interesting result is that all three methods, starting from the same FB, converge to almost identical synthesis FBs. The computation times are however very different: more than two hours (with $N = 16$) for the constrained optimization against a few seconds for the unconstrained optimizations. We can also notice that the gradient algorithm is as fast as the `fminunc` Matlab function. This shows that the optimization method can be easily implemented, through a gradient algorithm, with no performance loss and without having to resort to the `fminunc` Matlab function.[1] In other words, this last result indicates that in some applicative contexts in which Matlab is not available the optimization method can still be easily and efficiently implemented.

3) Examples of Optimized FBs: In this section, we present optimization results[2] obtained with the different FBs introduced in Section V-A and using the different proposed cost functions.

a) General case: We have applied the optimization method on the real FB introduced in Section V-A-1 with parameters: $N = 8$, $k = 4$ and $k' = 2$. The employed cost function is $\widetilde{J}_{\mathsf{t}}$. The result is shown in Fig. 4(b), the coefficients before optimization (obtained with the pseudoinverse method) are also displayed. It is clear that the impulse responses of optimized filters are better concentrated around the middle of the support. Fig. 3 illustrates that the gain in time localization does not entail a too severe loss in frequency selectivity of the optimized filters.

A second optimization example is given using an MCLT FB with analysis window h_{a_1} and parameters $N = 8$, $k = 3$ and $k' = 7/4$. The resulting frequency responses after optimization with cost function $\widetilde{J}_{\mathsf{f}}$ are represented in Fig. 5(b). We observe

[1]This fairly sophisticated function uses an interior-reflective Newton method [52].

[2]A Matlab toolbox for FB optimization is available here: http://www.laurent-duval.eu/misc-research-codes.html.

TABLE III
TIME DISPERSION OF THE SYNTHESIS FILTERS OPTIMIZED WITH COST FUNCTION $\widetilde{J}_{\mathsf{ts}}$

Filter	Time disp.	Filter	Time disp.
$\widetilde{h}_0$, $\widetilde{h}_{15}$	21.25	$\widetilde{h}_0^{opt}$, $\widetilde{h}_{15}^{opt}$	2.4152
$\widetilde{h}_1$, $\widetilde{h}_{14}$	21.25	$\widetilde{h}_1^{opt}$, $\widetilde{h}_{14}^{opt}$	2.1064
$\widetilde{h}_2$, $\widetilde{h}_{13}$	21.25	$\widetilde{h}_2^{opt}$, $\widetilde{h}_{13}^{opt}$	2.3424
$\widetilde{h}_3$, $\widetilde{h}_{12}$	21.25	$\widetilde{h}_3^{opt}$, $\widetilde{h}_{12}^{opt}$	2.5516
$\widetilde{h}_4$, $\widetilde{h}_{11}$	21.25	$\widetilde{h}_4^{opt}$, $\widetilde{h}_{11}^{opt}$	2.5516
$\widetilde{h}_5$, $\widetilde{h}_{10}$	21.25	$\widetilde{h}_5^{opt}$, $\widetilde{h}_{10}^{opt}$	2.3424
$\widetilde{h}_6$, $\widetilde{h}_9$	21.25	$\widetilde{h}_6^{opt}$, $\widetilde{h}_9^{opt}$	2.1064
$\widetilde{h}_7$, $\widetilde{h}_8$	21.25	$\widetilde{h}_7^{opt}$, $\widetilde{h}_8^{opt}$	2.4152
$\widetilde{J}_{\mathsf{ts}}$	340		37.6626

that the frequency responses after optimization exhibit more regularity and an improved selectivity. The proposed cost functions take into account all synthesis filters at once. It is therefore interesting to look more closely at each filter independently and determine whether the optimization leads to better results. In Table II, the frequency dispersion of each filter is reported before and after optimization with cost function $\widetilde{J}_{\mathsf{f}}$. In this case, the overall frequency dispersion of the optimized filters has been noticeably improved and spread variability has been drastically reduced.

b) Results in the symmetric case: The optimization procedure was next applied in the HS case to the FB of Section V-A-2 (with analysis window h_{a_2}). In this case, the cost functions $\widetilde{J}_{\mathsf{ts}}$ and $\widetilde{J}_{\mathsf{fs}}$ were employed. Once again, the following parameters were used: $N = 8$, $k = 3$ and $k' = 7/4$. Figs. 8 and 9 show the optimization results. We observe that the optimizations with these two cost functions lead to FBs with different characteristics: as expected, with $\widetilde{J}_{\mathsf{ts}}$ the impulse responses are better concentrated than with $\widetilde{J}_{\mathsf{fs}}$ and, conversely, with $\widetilde{J}_{\mathsf{fs}}$ the frequency selectivity is better than with $\widetilde{J}_{\mathsf{ts}}$.

4) Comparison: To conclude this example section, we propose a comparison with an existing filter bank design. We have chosen to compare our design methodology with the filter banks used in [4] and [7]. In these works, the considered FBs correspond to a modulated complex lapped transform with overlap factor $k = 2$ and redundancy $k' = 2$. For this application, our choice of $N = 8$ results in the filters shown in [4]. The synthesis filter bank is then built with a method equivalent to the weighted overlap-add technique. We have applied the methods proposed in this work to compute an optimized synthesis filter bank using the cost function $\widetilde{J}_{\mathsf{ts}}$. In Table III, the time dispersion of each synthesis filter computed as explained in [4] $(\widetilde{h}_j)_{j\in\{0,\ldots,15\}}$ and after optimization $(\widetilde{h}_j^{opt})_{j\in\{0,\ldots,15\}}$ are reported as well as the value of the cost function $\widetilde{J}_{\mathsf{ts}}$. The time dispersion was clearly reduced with the proposed method.

VI. CONCLUSION

In this paper, we have proposed a method to test that a given oversampled FIR analysis FB is FIR invertible and a method to compute an optimized inverse FB. The optimization was performed for a class of cost functions allowing either to emphasize the time localization or the frequency selectivity of the filters. By rewriting the system defining the synthesis FB, we were able to parameterize the synthesis filters for a given filter length. This parameterization was then used to convert the constrained optimal synthesis problem into an unconstrained one, which can be solved with a simple gradient algorithm.

The FB considered here are one-dimensional; it would be interesting to study how the proposed methods could be extended to the multidimensional case. Another perspective could be to study the case of FBs admitting an IIR left inverse that can be approximated using a FIR FB with very long support.

APPENDIX A
EXPRESSION OF THE GRADIENT

In this first appendix, we study the gradient of $\widetilde{J}$ (as defined in Section IV-B-1) with respect to $\mathcal{C}$. We first need to calculate the gradient of $f(\mathcal{C}) = \|\boldsymbol{V}_j\mathcal{C} + \widetilde{\boldsymbol{H}}_j^0\|_{K_j}^2$. The matrix $\mathcal{C}$ being complex, we have

$$\begin{aligned}
&\frac{\partial f}{\partial \mathcal{C}_{m,n}} \\
&\quad = \frac{\partial f}{\partial \mathcal{C}_{m,n}^R} + \imath\frac{\partial f}{\partial \mathcal{C}_{m,n}^I} \\
&\quad = \sum_{i,i',\ell,\ell'} K_j(i,i',\ell,\ell') \\
&\qquad \times \left((\boldsymbol{V}_j)_{i,m}\delta_{\ell-n}\left(\overline{\boldsymbol{V}_j\mathcal{C} + \widetilde{\boldsymbol{H}}_j^0}\right)_{i',\ell'} + \overline{(\boldsymbol{V}_j)}_{i',m}\delta_{\ell'-n} \right. \\
&\qquad\qquad \left. \times \left(\boldsymbol{V}_j\mathcal{C} + \widetilde{\boldsymbol{H}}_j^0\right)_{i,\ell}\right) + \imath K_j(i,i',\ell,n) \\
&\qquad \times \left(\imath(\boldsymbol{V}_j)_{i,m}\delta_{\ell-n}\overline{(\boldsymbol{V}_j\mathcal{C} + \widetilde{\boldsymbol{H}}_j^0)}_{i',\ell'} \right. \\
&\qquad\qquad \left. -\imath\overline{(\boldsymbol{V}_j)}_{i',m}\delta_{\ell'-n}(\boldsymbol{V}_j\mathcal{C} + \widetilde{\boldsymbol{H}}_j^0)_{i,\ell}\right) \\
&\quad = 2\sum_{i,i',\ell} (\overline{\boldsymbol{V}_j})_{i',m}(\boldsymbol{V}_j\mathcal{C} + \widetilde{\boldsymbol{H}}_j^0)_{i,\ell}.
\end{aligned}$$

From this result, we deduce that

$$\begin{aligned}
\left(\nabla\widetilde{J}(\mathcal{C})\right)_{m,n} = \sum_{j=0}^{M-1}\frac{2}{\beta_j^2}\sum_{i,i',\ell}(\overline{\boldsymbol{V}_j})_{i',m}\left(\boldsymbol{V}_j\mathcal{C} + \widetilde{\boldsymbol{H}}_j^0\right)_{i,\ell} \\
\times\left(\beta_j K_j(i,i',\ell,n) - \alpha_j\Lambda(i,i',\ell,n)\right), \quad (23)
\end{aligned}$$

with $\alpha_j = \|\boldsymbol{V}_j\mathcal{C} + \widetilde{\boldsymbol{H}}_j^0\|_{K_j}^2$ and $\beta_j = \|\boldsymbol{V}_j\mathcal{C} + \widetilde{\boldsymbol{H}}_j^0\|_{\Lambda}^2$.

APPENDIX B
EXAMPLES OF GRADIENTS

A first example is the calculation of the gradient of the cost function $\widetilde{J}_{\mathsf{t}}$. Applying (23) to the kernels $(K_j^{\mathsf{t}})_{0\le j<M}$, we get:

$$\begin{aligned}
\frac{\partial f}{\partial \mathcal{C}_{m,n}} &= 2\omega_{\mathsf{t},j}\sum_i(\overline{\boldsymbol{V}_j})_{i,m}\left(\boldsymbol{V}_j\mathcal{C} + \widetilde{\boldsymbol{H}}_j^0\right)_{i,n}(\boldsymbol{\Gamma}_j)_{i,n} \\
&= 2\omega_{\mathsf{t},j}\left(\boldsymbol{V}_j^*\left(\boldsymbol{\Gamma}_j\odot\left(\boldsymbol{V}_j\mathcal{C} + \widetilde{\boldsymbol{H}}_j^0\right)\right)\right)_{m,n},
\end{aligned}$$

where $(\mathbf{\Gamma}_j)_{i,\ell+p_1} = |\ell N - i - \overline{m}_j|^\alpha$ for all $0 \leq i < N$ and $-p_1 < \ell \leq p_2$. The symbol $\odot$ represents the Hadamard product (or pointwise matrix product). Finally we obtain:

$$\nabla \widetilde{J}_{\mathsf{t}}(\mathcal{C}) = 2 \sum_{j=0}^{M-1} \frac{\boldsymbol{V}_j^* \left((\omega_{\mathsf{t},j} \beta_j \mathbf{\Gamma}_j - \alpha_j \mathbf{1}) \odot \left(\boldsymbol{V}_j \mathcal{C} + \widetilde{\boldsymbol{H}}_j^0 \right) \right)}{\beta_j^2},$$

where $\mathbf{1}_{i,\ell} = 1$ for all $0 \leq i < N$ and $0 \leq \ell < p$.

The same study can be carried out for the cost function $\widetilde{J}_{\mathsf{f}}$, with kernels $(K_j^{\mathsf{f}})_{0 \leq j < M}$. Rewriting the result under a matrix form does not simplify the final expression in this case. Hence, the gradient reads:

$$\left(\nabla \widetilde{J}_{\mathsf{t}}(\mathcal{C}) \right)_{m,n} = \sum_{j=0}^{M-1} \frac{2}{\beta_j^2} \sum_{i,i',\ell} (\overline{\boldsymbol{V}_j})_{i',m} \left(\boldsymbol{V}_j \mathcal{C} + \widetilde{\boldsymbol{H}}_j^0 \right)_{i,\ell} \times (\beta_j K_j^{\mathsf{f}}(i,i',\ell,n) - \alpha_j \delta_{i-i'} \delta_{\ell-n}).$$

Appendix C
Gradient Functions in the HS Case

Similarly to Appendix A, we first compute the gradient of $f(\mathcal{C}) = \|\boldsymbol{W}_j \mathcal{C} + \widetilde{\boldsymbol{H}}_j^0\|_{K_j}^2$ with respect to the matrix $\mathcal{C}$, the only difference being that the matrix $\mathcal{C}$ is now real:

$$\frac{\partial f}{\partial \mathcal{C}_{m,n}} = \sum_{i,i',\ell,\ell'} \left((\boldsymbol{W}_j)_{i,m} \delta_{\ell-n} \left(\overline{\boldsymbol{W}_j \mathcal{C} + \widetilde{\boldsymbol{H}}_j^0} \right)_{i',\ell'} + (\overline{\boldsymbol{W}_j})_{i',m} \delta_{\ell'-n} \left(\boldsymbol{W}_j \mathcal{C} + \widetilde{\boldsymbol{H}}_j^0 \right)_{i,\ell} \right) K_j(i,i',\ell,\ell').$$

By using this expression and the relation $K_j(i,i',\ell,\ell') = \overline{K_j(i',i,\ell',\ell)}$, we deduce the gradient of the cost function $\widetilde{J}_{\mathsf{s}}$:

$$\left(\nabla \widetilde{J}_{\mathsf{s}}(\mathcal{C}) \right)_{m,n} = \mathrm{Re} \left(\sum_{j=0}^{M-1} \sum_{i,i',\ell'} (\boldsymbol{W}_j)_{i,m} \left(\overline{\boldsymbol{W}_j \mathcal{C} + \widetilde{\boldsymbol{H}}_j^0} \right)_{i',\ell'} \times \frac{2}{\beta_j^2} \left(\beta_j K_j(i,i',n,\ell') - \alpha_j \Lambda(i,i',n,\ell') \right) \right), \quad (24)$$

with $\alpha_j = \|\boldsymbol{W}_j \mathcal{C} + \widetilde{\boldsymbol{H}}_j^0\|_{K_j}^2$ and $\beta_j = \|\boldsymbol{W}_j \mathcal{C} + \widetilde{\boldsymbol{H}}_j^0\|_{\Lambda}^2$, for all $0 \leq j < M$. Using (24), the calculation of the gradient of $\widetilde{J_{\mathsf{ts}}}$ yields

$$\nabla \widetilde{J_{\mathsf{ts}}}(\mathcal{C}) = 2\mathrm{Re} \left(\sum_{j=0}^{M-1} \frac{\boldsymbol{W}_j^* \left((\omega_{\mathsf{t},j} \beta_j \mathbf{\Gamma}_j - \alpha_j \mathbf{1}) \odot \left(\boldsymbol{W}_j \mathcal{C} + \widetilde{\boldsymbol{H}}_j^0 \right) \right)}{\beta_j^2} \right),$$

where $\mathbf{\Gamma}_j$ is defined as in Appendix B. For the second cost function we find

$$\left(\nabla \widetilde{J_{\mathsf{fs}}}(\mathcal{C}) \right)_{m,n} = \mathrm{Re} \left(\sum_{j=0}^{M-1} \sum_{i,i',\ell'} (\boldsymbol{W}_j)_{i,m} \left(\overline{\boldsymbol{W} \mathcal{C} + \widetilde{\boldsymbol{H}}_j^0} \right)_{i',\ell'} \times \frac{2}{\beta_j^2} \left(\beta_j K_j^{\mathsf{f}}(i,i',n,\ell') - \alpha_j \delta_{i-i'} \delta_{n-\ell'} \right) \right).$$

Acknowledgment

The authors would like to thank the reviewers and the Associate Editor for their valuable comments and suggestions. They also wish to thank Dr. Stefan Weiß for useful references.

References

[1] W. Kellermann, "Analysis and design of multirate systems for cancellation of acoustical echoes," in *Proc. Int. Conf. Acoust., Speech, Signal Process.*, New York, Apr. 11–14, 1988, pp. 2570–2573.
[2] H. Bölcskei and F. Hlawatsch, "Oversampled cosine modulated filterbanks with perfect reconstruction," *IEEE Trans. Circuits Syst. II*, vol. 45, no. 8, pp. 1057–1071, Aug. 1998.
[3] F. Labeau, J.-C. Chiang, M. Kieffer, P. Duhamel, L. Vandendorpe, and B. Macq, "Oversampled filter banks as error correcting codes: Theory and impulse noise correction," *IEEE Trans. Signal Process.*, vol. 53, no. 12, pp. 4619–4630, Dec. 2005.
[4] R. W. Young and N. G. Kingsbury, "Frequency-domain motion estimation using a complex lapped transform," *IEEE Trans. Image Process.*, vol. 2, no. 1, pp. 2–17, Jan. 1993.
[5] H. Bölcskei, F. Hlawatsch, and H. G. Feichtinger, "Frame-theoretic analysis of oversampled filter banks," *IEEE Trans. Signal Process.*, vol. 46, no. 12, pp. 3256–3268, Dec. 1998.
[6] Z. Cvetković and M. Vetterli, "Overampled filter banks," *IEEE Trans. Signal Process.*, vol. 46, no. 5, pp. 1245–1255, May 1998.
[7] H. S. Malvar, "A modulated complex lapped transform and its applications to audio processing," in *Proc. Int. Conf. Acoust., Speech, Signal Process.*, Phoenix, AZ, Mar. 1999, vol. 3, pp. 1421–1424.
[8] H. Bölcskei and F. Hlawatsch, "Oversampled filter banks: Optimal noise shaping, design freedom, and noise analysis," in *Proc. IEEE Int. Conf. Acoust., Speech, Signal Process.*, Apr. 21–24, 1997, vol. 3, pp. 2453–2456.
[9] V. K. Goyal, J. Kovačević, and J. A. Kelner, "Quantized frame expansions with erasures," *Appl. Comp. Harmon. Anal.*, vol. 10, no. 3, pp. 203–233, May 2001.
[10] B. Dumitrescu, R. Bregović, and T. Saramäki, "Simplified design of low delay oversampled NPR GDFT filterbanks," in *EURASIP J. Appl. Signal Process.*, 2006, vol. 2006, p. 11.
[11] B. Hassibi, B. Hochwald, A. Shokrollahi, and W. Sweldens, "Representation theory for high-rate multiple-antenna code design," *IEEE Trans. Inf. Theory*, vol. 47, no. 6, pp. 2355–2367, Sep. 2001.
[12] K. S. C. Pun and T. Q. Nguyen, "Design of oversampled filter bank-based widely linear OQPSK equalizer," in *Proc. IEEE Int. Conf. Acoust., Speech, Signal Process.*, Honolulu, HI, Apr. 15–20, 2007, vol. 3, pp. 861–864.
[13] T. Ihalainen, T. H. Stitz, M. Rinne, and M. Renfors, "Channel equalization in filter bank based multicarrier modulation for wireless communications," in *EURASIP J. Appl. Signal Process.*, 2007, vol. 2007, p. 18.
[14] H. Johansson and P. Löwenborg, "Flexible frequency-band reallocation networks using variable oversampled complex-modulated filter banks," in *EURASIP J. Appl. Signal Process.*, 2007, vol. 2007, p. 15.
[15] S. Weiß, S. Redif, T. Cooper, C. Liu, P. D. Baxter, and J. G. McWhirter, "Paraunitary oversampled filter bank design for channel coding," in *EURASIP J. Appl. Signal Process.*, 2006, vol. 2006, p. 10.
[16] Z. Cvetković and M. Vetterli, "Tight Weyl-Heisenberg frames in $\ell^2(\mathbb{R})$," *IEEE Trans. Signal Process.*, vol. 46, no. 5, pp. 1256–1259, May 1998.
[17] K. F. C. Yui, N. Grbić, S. Nordholm, and K. L. Teo, "Multicriteria design of oversampled uniform DFT filter banks," *Signal Process. Lett.*, vol. 11, no. 6, pp. 541–544, Jun. 2004.
[18] N.-T. Ueng and L. L. Scharf, "Frames and orthonormal bases for variable windowed Fourier transforms," in *Proc. Int. Conf. Acoust., Speech, Signal Process.*, Atlanta, GA, May 7–10, 1996, vol. 5, pp. 2594–2597.
[19] R. von Borries, R. de Queiroz, and C. S. Burrus, "On filter banks with rational oversampling," in *Proc. IEEE Int. Conf. Acoust., Speech, Signal Process.*, Salt Lake City, UT, May 7–11, 2001, vol. 6, pp. 3657–3660.
[20] R. von Borries and C. S. Burrus, "Linear phase oversampled filterbanks," in *Proc. IEEE Int. Conf. Acoust., Speech Signal Process.*, Montreal, QC, Canada, May 17–21, 2004, vol. 2, pp. 961–964.

[21] L. Gan and K.-K. Ma, "Oversampled linear-phase perfect reconstruction filter banks: Theory, lattice structure and parameterization," *IEEE Trans. Signal Process.*, vol. 51, no. 3, pp. 744–759, Mar. 2003.
[22] T. Tanaka, "A direct design of oversampled perfect reconstruction FIR filter banks of 50%-overlapping filters," *IEEE Trans. Signal Process.*, vol. 54, no. 8, pp. 3011–3022, Aug. 2006.
[23] B. Riel, D. J. Shpak, and A. Antoniou, "Lifting-based design and implementation of oversampled paraunitary modulated filter banks," in *Proc. Mid. Symp. Circuits Syst.*, Hiroshima, Japan, Jul. 25–28, 2004, vol. 2, pp. 97–100.
[24] M. Harteneck, S. Weiß, and R. Stewart, "Design of near perfect reconstruction oversampled filter banks for subband adaptive filters," *IEEE Trans. Circuits Syst. II*, vol. 46, no. 8, pp. 1081–1086, Aug. 1999.
[25] M. R. Wilbur, T. Davidson, and J. P. Reilly, "Efficient design of oversampled NPR GDFT filter banks," McMaster Univ., Hamilton, ON, Canada, Tech. Rep., Jul. 2003.
[26] D. Hermann, E. Chau, R. D. Dony, and S. M. Areibi, "Window based prototype filter design for highly oversampled filter banks in audio applications," in *Proc. IEEE Int. Conf. Acoust., Speech Signal Process.*, Honolulu, HI, Apr. 15–20, 2007, vol. 2, pp. 405–408.
[27] T. Kalker, H. Park, and M. Vetterli, "Groebner basis techniques in multidimensional multirate systems," in *Proc. Int. Conf. Acoust., Speech, Signal Process.*, Detroit, MI, May 9–12, 1995, vol. 4, pp. 2121–2124.
[28] H. Park, T. Kalker, and M. Vetterli, "Gröbner bases and multidimensional FIR multirate systems," *Multidimension. Syst. Signal Process.*, vol. 8, pp. 11–30, Jan. 1997.
[29] J. Zhou and M. N. Do, "Multidimensional oversampled filter banks," in *Proc. SPIE, Wavelets Appl. Signal Image Process.*, M. Papadakis, A. F. Laine, and M. A. Unser, Eds., San Diego, CA, Jul. 31–Aug. 3 2005, vol. 5914, pp. 591 424.1–591 424.12.
[30] L. Chai, J. Zhang, C. Zhang, and E. Mosca, "Frame-theory-based analysis and design of oversampled filter banks: Direct computational method," *IEEE Trans. Signal Process.*, vol. 55, no. 2, pp. 507–519, Feb. 2007.
[31] F. Labeau, "Synthesis filters design for coding gain in oversampled filter banks," *Signal Process. Lett.*, vol. 12, no. 10, pp. 697–700, Oct. 2005.
[32] M. F. Mansour, "On the optimization of oversampled DFT filter banks," *Signal Process. Lett.*, vol. 14, no. 6, pp. 389–392, Jun. 2007.
[33] J. Gauthier, L. Duval, and J. C. Pesquet, "Low redundancy oversampled lapped transforms and application to 3D seismic data filtering," in *Proc. IEEE Int. Conf. Acoust., Speech, Signal Process.*, Toulouse, France, May 2006, vol. 2, pp. 821–824.
[34] J. Gauthier, L. Duval, and J. C. Pesquet, "Oversampled inverse complex lapped transform optimization," in *Proc. IEEE Int. Conf. Acoust., Speech, Signal Process.*, Honolulu, HI, Apr. 2007, vol. 1, pp. 549–552.
[35] E. Fornasini and M. E. Valcher, "nD polynomial matrices with applications to multidimensional signal analysis," *Multidimension. Syst. Signal Process.*, vol. 8, pp. 387–408, Oct. 1997.
[36] H. Park, "Symbolic computation and signal processing," *J. Symb. Comput.*, vol. 37, no. 2, pp. 209–226, Feb. 2004.
[37] A. Ben-Israel and T. N. E. Greville, *Generalized Inverses: Theory and Applications*, 2nd ed. New York: Springer-Verlag, 2003.
[38] T. Tanaka and Y. Yamashita, "The generalized lapped pseudobiorthogonal transform: Oversampled linear-phase perfect reconstruction filter banks with lattice structures," *IEEE Trans. Signal Process.*, vol. 52, no. 2, pp. 434–446, Feb. 2004.
[39] S. Komeiji and T. Tanaka, "A direct design of oversampled perfect reconstruction bandpass FIR filterbanks with real coefficients," in *Proc. RISP Int. Workshop on Nonlinear Circuits Signal Process. (NCSP)*, Shanghai, China, Mar. 2007, pp. 611–614.
[40] H. S. Malvar, *Signal Processing with Lapped Transforms*. Norwood, MA: Artech House, 1992.
[41] P. M. Cassereau, D. H. Staelin, and G. De Jager, "Encoding of images based on lapped orthogonal transform," *IEEE Trans. Commun.*, vol. 37, no. 2, pp. 189–193, Feb. 1989.
[42] P. P. Vaidyanathan, *Multirate Systems and Filter Banks*. Englewood Cliffs, NJ: Prentice-Hall, 1993.
[43] T. Kailath, *Linear Systems*. Englewood Cliffs, NJ: Prentice-Hall, 1980.
[44] G. D. Forney, "Minimal bases of rational vector spaces, with applications to multivariable linear systems," *SIAM J. Control Optim.*, vol. 13, no. 3, pp. 493–520, May 1975.
[45] Y. Inouye and R. W. Liu, "A system-theoretic foundation for blind equalization of an FIR MIMO channel system," *IEEE Trans. Circuits Syst. I*, vol. 49, no. 4, pp. 425–436, Apr. 2002.
[46] R. Penrose, "A generalized inverse for matrices," in *Proc. Camb. Philos. Soc.*, 1955, vol. 51, pp. 406–413.
[47] G. Strang, *Introduction to Linear Algebra*, 2nd ed. Wellesley, MA: Wellesley-Cambridge, 1998.
[48] P. Flandrin, *Time-Frequency and Time-Scale Analysis*. San Diego, CA: Academic, 1998.
[49] J. Nocedal and S. J. Wright, *Numerical Optimization*. New York: Springer-Verlag, 1999.
[50] M. Barrault and C. Le Bris, Optimisation numérique et différentiation automatique pour un problème industriel Rapports de Recherche du CERMICS, Champs-sur-Marne, Tech. Rep., Oct. 1999.
[51] R. de Queiroz, T. Nguyen, and K. Rao, "The GenLOT: generalized linear-phase lapped orthogonal transform," *IEEE Trans. Signal Process.*, vol. 44, no. 3, pp. 497–507, Mar. 1996.
[52] T. F. Coleman and Y. Li, "On the convergence of interior-reflective Newton methods for nonlinear minimization subject to bounds," *Math. Programm.*, vol. 67, no. 2, pp. 189–224, 1994.

Jérôme Gauthier (S'08–M'08) was born in Rouen, France, in 1980. In 2004, he received the D.E.A. degree in analysis and stochastic models from the Université de Rouen, France, and the Ph.D. degree in signal and image processing from the Laboratoire d'Informatique (UMR-CNRS 8049) of the Université Paris-Est, France, on the topic of filter banks construction and optimization and their applications to Geosciences.

Since June 2008, he holds a postdoctoral position within the Signal and Image Processing Department of Telecom ParisTech, France, on the topic of Distributed Video Coding.

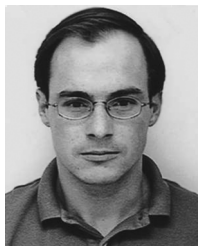

Laurent Duval (S'98–M'01) was born in Cherbourg, France. He received the State Engineering degree in electrical engineering from Supélec, Gif-sur-Yvette, France, the Diplôme d'Études Approfondies (D.E.A.) degree in pure and applied mathematics from the Université Paul Verlaine Metz, France, in 1996, and the Ph.D. degree in signal processing from the Université Paris-Sud XI, Orsay, France, in 2000, on the topic of seismic data compression.

In 1998, he worked as a Research Assistant in the Multi-Dimensional Signal Processing Laboratory (MDSP Lab) at Boston University, Boston, MA. In April 2000, he joined the Institut Français du Pétrole (IFP), Rueil-Malmaison, France, as a Research Engineer. He now conducts research in signal and image processing with application to geosciences, material characterization, chemical analysis, and engine control. His research interests are in the area of digital signal and image processing, with a special emphasis on filter bank techniques and their applications in signal detection, filtering, and data compression.

Jean-Christophe Pesquet (S'89–M'91–SM'99) received the engineering degree from Supélec, Gif-sur-Yvette, France, in 1987, the Ph.D. degree from the Université Paris-Sud (XI), Paris, France, in 1990, and the Habilitation à Diriger des Recherches from the Université Paris-Sud in 1999.

From 1991 to 1999, he was a Maître de Conférences with the Université Paris-Sud, and a Research Scientist with the Laboratoire des Signaux et Systèmes, Centre National de la Recherche Scientifique (CNRS), Gif sur Yvette. He is currently a Professor with the Université de Paris-Est Marne-la-Vallée, France, and a Research Scientist with the Laboratoire d'Informatique of the University (UMR–CNRS 8049).